DANMARKS OG GRØNLANDS GEOLOGISKE UNDERSØGELSE RAPPORT 2015/92

Water4Coast

Modelling the effects of hydraulic barriers to control saltwater intrusion in a coastal chalk aquifer

Per Rasmussen, Torben O. Sonnenborg
& Klaus Hinsby

GEOLOGICAL SURVEY OF DENMARK AND GREENLAND
DANISH MINISTRY OF CLIMATE, ENERGY AND BUILDING

G E U S

DANMARKS OG GRØNLANDS GEOLOGISKE UNDERSØGELSE RAPPORT 2015/92

Water4Coasts

Modelling the effects of hydraulic barriers to control saltwater intrusion in a coastal chalk aquifer

Per Rasmussen, Torben O. Sonnenborg
& Klaus Hinsby

GEOLOGICAL SURVEY OF DENMARK AND GREENLAND
DANISH MINISTRY OF ENERGY,UTILITIES AND CLIMATE

G E U S

Table of contents

1. Summary and Conclusions

Coastal aquifers are at risk of saltwater intrusion. This is a well described problem from many coastal areas and from coastal areas with limited access to other freshwater resources. Hydraulic barriers are one technique to protect the coastal aquifers from saltwater intrusion, e.g. with injection wells creating an artificial groundwater divide between the seawater and the groundwater aquifer by injection of water into the subsurface.

Groundwater models including variable density flow can be used to evaluate the effects of different types and configurations of hydraulic barriers. Geophysical data like borehole logging and geophysical surveys can be used to improve the calibration of groundwater models.

The possible effects of using injection wells as hydraulic barrier against salt water intrusion have been tested with an existing groundwater model for the Marielyst area on Falster, and with generic models.

Geophysical data have been interpreted and implemented in the groundwater model in order to improve the model calibration. The pilot point calibration technique has also been tested for the study area in Marielyst, Falster.

The results of the pilot point test calibration suggest that it could be valuable to implement the more heterogenetic distribution of hydraulic conductivities found in the pilot point calibration.

Various configurations and pumping rates for injection wells have been tested. The model studies have shown that e.g. a horizontal well with a length of 150 m injecting 1/3 of the water injected by three vertical wells with horizontal spacing of 300 m have a larger effect on preventing seawater intrusion. With a large vertical spacing between vertical injection wells a lot of injected water may be wasted.

The test of different injection well setups with generic models indicates that the injection rate is of most importance in heterogeneous aquifers.

Monitoring wells should be deep enough to be able to measure the changes in seawater intrusion below the freshwater lens. Monitoring wells should have monitoring points at different depth in the aquifer.

The modelling results show a large potential of hydraulic barriers and injection wells for controlling salt water intrusion and protection of coastal freshwater resources. However, further and more detailed investigations of the hydraulic parameters and geochemistry of the Chalk aquifer on Southern Falster is needed in order to further explore and define the possible and most efficient subsurface solutions for controlling salt water intrusion around the water supply wells of the Marielyst water works.

The upper part of the exploited Chalk aquifer has been strongly affected by several glaciations and glaciotectonics, and the hydraulic properties vary significantly. Hence, focused and detailed investigations at the water supply wells are needed in order to identify the best and most efficient options for controlling salt water intrusion and protecting the freshwater resources including the design and location of potential injection and abstraction wells.

The investigations on the use of managed aquifer recharge and other subsurface solutions on Falster, Denmark initiated in the Water4Coasts project is currently continued in the 'SubSol' project: 'Bringing coastal SUBsurface water SOLutions to the market' (European Commission, 2015a) in 'Horizon 2020' - the research and innovation program of the European Commission (European Commission, 2015b). A project flyer, results and updates on the progress of this project can be found on the project website: www.subsol.org.

2. Introduction

Background

Coastal aquifers are at risk of saltwater intrusion which may reduce or even preclude groundwater abstraction for water supply from these aquifers. This is a well described problem from many densely populated coastal areas and from coastal areas with limited access to other freshwater resources, e.g. minor islands. Climate change is likely to result in increasing sea levels which again may increase the risk of saltwater intrusion to coastal groundwater aquifers.

Hydraulic barriers are one technique to protect the coastal aquifers from (increasing) saltwater intrusion. Hydraulic barriers can be established in several ways, e.g. with injection wells creating an artificial groundwater divide between the seawater and the groundwater aquifer by injection of water into the subsoil. Other methods include multiple wells abstraction controlling the freshwater-saltwater interface (Zuurbier et al. 2014), negative hydraulic barriers (Pool and Carrera 2010), or installing impermeable walls between the saltwater and the fresh groundwater aquifer (Kaleris and Ziogas 2013).

One method to evaluate the effects of different types and configurations of hydraulic barriers is to use groundwater models which include transient and variable density flow domains. Besides measurements of groundwater heads and stream discharges, geophysical borehole logging, geophysical surveys and groundwater quality data can be used to improve the calibration of the variable density groundwater model.

Previous studies

Several studies have recommended the use of geophysical data to improve the calibration of variable density groundwater models. Geo-electrical inversion models of the sub-surface and variable density groundwater models can be cross-validated and thereby improve the modelling of saltwater intrusion (Comte and Banton, 2007). Carrera et al. (2010) stated that model calibration can be improved significantly by including the airborne geophysical measurements in the calibration process.

Another method of improving the model calibration is by using the pilot point technique where the spatial variations in hydraulic conductivities can be determined (Christensen and Doherty, 2008; Dausman et al., 2010; Langevin and Zygnerski, 2013; Maneta and Wallender, 2013).

Injection wells used as hydraulic barriers to prevent (further) saltwater intrusion may (also) act as an ASR (Artificial Storage and Recovery) system where part of the injected water (may possibly) end up in the abstraction wells (David and Pyne 2005). Ward et al. (2008 and 2009) analyses the effects of lateral flow, density-driven flow, dispersive mixing, discontinuities in pumping, and anisotropic and layered heterogeneous aquifers on ASR systems.

Misut and Voss (2007) found through model studies that freshwater storage by injection followed by phases of pause and recovery by extraction may benefit coastal water users if less water is recovered than injected and thereby establishing a hydraulic saltwater intrusion barrier.

This study
WATER4COASTS Activity 1.2 includes saltwater intrusion and freshwater injection modelling. A calibrated saltwater intrusion model (SWI) already exists for the Danish study site on the island of Falster (Rasmussen et al., 2013). New airborne geophysical data collected for the Danish Nature Agency has become available since the calibration of the existing model. Also a new investigation borehole has provided new geological and geophysical data.

The first phase of this activity includes the recalibration of the existing model based on new airborne geophysical data and new data from geophysical borehole logging. Pilot point calibration is tested to see if it improves the model performance. In the second phase the recalibrated model are used to analyse the effect of different configurations and management strategies of injections wells.

The chemical, biological and pollution aspects of injecting surface water into the groundwater aquifer are dealt with under Activity 1.3 and 1.4.

Activity 1.2 includes 2 milestones, M1: Falster model calibrated and validated and M3: Required well injection in different injection designs and scenarios simulated by model.

WATER4COASTS Activity 2.2 includes the development of generic saltwater / freshwater models to illustrate the general effects of various types of hydraulic barriers under various hydrogeological and climate scenarios.

Generic models can be applied to assess different designs of hydraulic barriers for relevant hydrogeological and climatological settings representing current and future climate settings for different global regions including projected climate change. Based on existing systems and literature different injection designs will be developed and evaluated by the generic models. Monitoring system designs will be proposed for monitoring the future evolution of groundwater and surface water quantity and quality during artificial aquifer recharge. This will include new technical solutions for monitoring groundwater and surface water chloride and nitrate concentrations (e.g. Thorn and Mortensen, 2012; Sulzbacher et al., 2012).

Activity 2.2 includes 1 milestone, M6: Generic model simulations completed.

The results of Activity 1.2 and 2.2 are both described in the present report.

The SWIM23 conference held in Husum in June 2014 offered an opportunity to present WATER4COASTS project Activity 1.2. A scenario with the existing model showing the effect of three injection wells in a changing climate on the water quality in two groundwater abstraction wells was presented (Appendix 1 and 2).

3. Methods

3.1 Study area

The study site is located in the south-eastern part of Denmark on the island of Falster. Towards the east the study area is bounded by the Baltic Sea and towards the west of the strait of Guldborgsund. The local waterworks are abstracting groundwater from the shallow chalk aquifer overlain by quaternary and post glacial sediments of mainly clayey tills and sands. The well fields located closest to the Baltic Sea coast have seen an increasing chloride concentration in the abstracted groundwater during the last decades (Figure 3-1).

The mean annual precipitation is around 700 mm/year, and the groundwater recharge has been estimated to 250 mm/year. The total groundwater abstraction in the area is 400,000 m^3/year or less than 5 % of the recharge. The main discharge from the area is through the pumping station downstream at the Marrebæk canal (Figure 3-1).

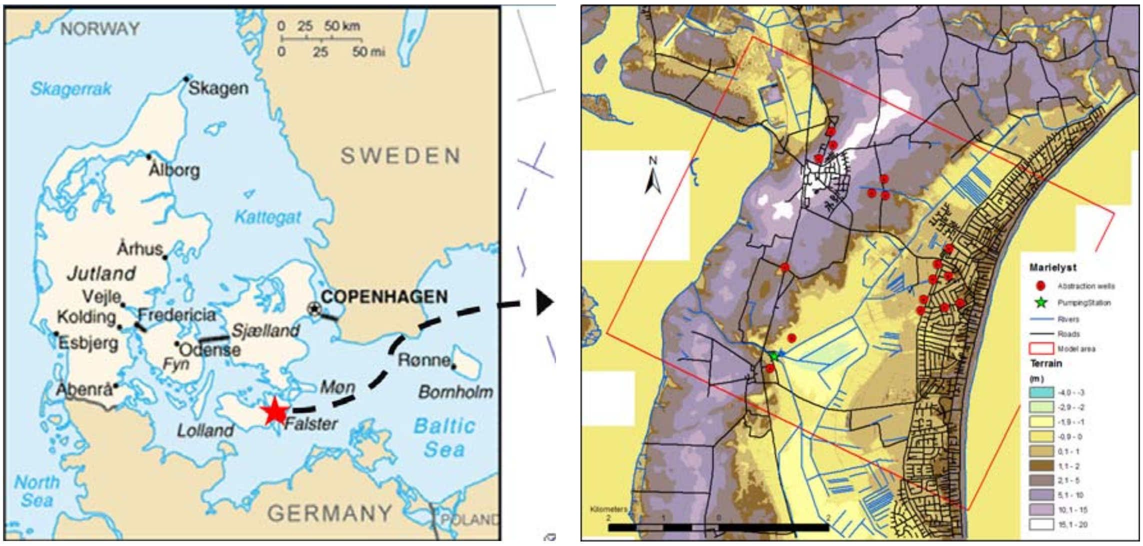

Figure 3-1. Location of study area, abstraction wells, drainage canal and pumping station

3.2 Data collection

Existing hydrogeological data from the study area are retrieved from the National well database (Jupiter), the National geophysical database (GERDA), the Groundwater reports database, and the Groundwater model database. During the last 15 years a special effort has been done to file existing data and to collect new data as part of the Danish Groundwater Mapping.

3.2.1 Groundwater chemistry

In the study area it is assumed that there are three potential sources for the salinity measured in groundwater abstraction wells; diffusion and/or upconing from deeper layers, interglacial/post glacial saltwater trapped in glacial/post glacial deposits, and seawater intrusion.

Groundwater chemistry data from selected existing groundwater abstraction wells were obtained from Marielyst Waterworks, the National well database (Jupiter), and from a previous project in the area, BaltCICA (http://www.baltcica.org/).

The molar ratio of sodium to chloride [Na]/[Cl] is an indication the origin of the salinization in a well. If the ratio is below 0.9 the salinization is most likely to come from seawater intrusion, whereas if the ratio is above 0.9 diffusion of connate saline water is the most like source of chloride (Appelo and Postma 2005, Thorn 2011).

Measurements of groundwater salinity and geophysical measurements can be linked and converted through well documented relationships and conversion factors, e.g. Archie's law (Larsen et al., 2006, Klitten and Wittrup, 2006, Rasmussen et al. 2013).

The most common parameters when dealing with the groundwater chemistry and geophysics are chloride concentrations, total dissolved solids concentrations (TDS), fluid resistivity and conductivity, bulk resistivity and conductivity, and the formation factor.

3.2.2 New research borehole, geological data

A new 45 m deep investigation borehole was established between the waterworks old well field and the Baltic Sea 150 m from the coast line, borehole no. 242.375 (Figure 3-2).

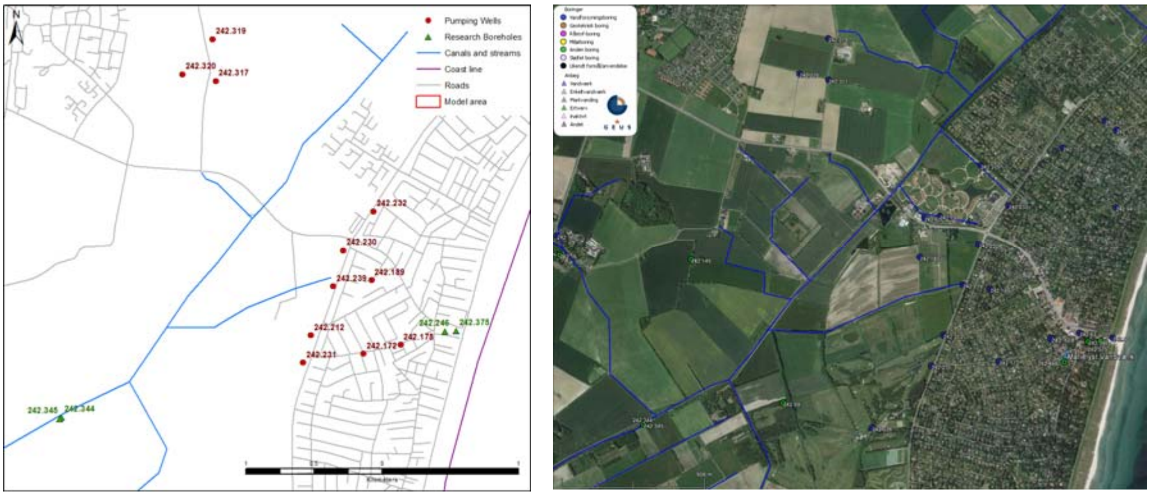

Figure 3-2. Location of reach boreholes and groundwater abstraction wells

Cores and soil samples were taken for a detailed lithological and stratigraphical description of the hydrogeological setting. Soil samples were collected for each one meter and detailed

described in the soil lab. Also a soil core was collected from a minor section of the borehole (Appendix 3).
The borehole was completed with a PVC screen from approximately 2 m above the top of the chalk formation to the bottom of the borehole. The reason for installing a screen in the chalk borehole was to be able to analyse groundwater flow conditions in the uppermost part of the chalk and in the zone between the chalk and the overlaying quaternary deposits.

3.2.3 Borehole geophysics, wireline logging

Borehole geophysics using wireline logging was carried out in the new investigation borehole with the purpose of getting more information of the groundwater flow in the fractured chalk aquifer with focus on the zone between the chalk aquifer and the overlaying quaternary deposit. The existing wells in the area, mainly groundwater abstractions wells, are all completed with an iron casing finishing 2-5 meters below the top of the chalk and are open boreholes 10 – 15 meters into the chalk. It is expected that the uppermost parts of the chalk is highly fractured or crushed resulting in a high hydraulic conductivity. The second focus point of the borehole logging is in the deepest part of the borehole with the transition zone above which advective groundwater flow is dominating and the saltwater is flushed out. Below the advective zone diffusion is becoming a more dominant process and saltwater is present in higher concentrations in the formation.

Borehole geophysics from the 100 m deep research borehole (242.344) is reported in Rasmussen et al. (2013).The following wireline logging data are collected from the research boreholes: Natural gamma, formation conductivity (induction log), fluid temperature and conductivity, and propeller flow log. Temperature/conductivity and flow logs are measured under two pumping conditions, no pumping and during constant groundwater abstraction.

3.2.4 Airborne geophysics and MEP

During the recent national groundwater mapping activities part of the study area was covered with airborne electromagnetics (AEM) by the Danish SkyTEM company. The Danish Nature Agency supported the data collection. The Aarhus Workbench software was used for handling, processing, and inversion of the resistivity measurements (Naturstyrelsen Roskilde, 2011).

One limitation of the AEM is that it cannot record resistivities in built-up areas due to power lines and cables. In the study area there is a high density of summerhouses along the east coast, which mean that no SkyTEM data are available from this area. Two of the well fields are located in the area with high density of summerhouses. The SkyTEM data was mainly collected in the central part of the study area, but not around two well fields and along the eastern coast line. 50 km of flight lines with a distance of 150-200 m were carried out. 17 km^2 has been covered with SkyTEM surveys out of the 44 km^2 study area (Figure 3-3).

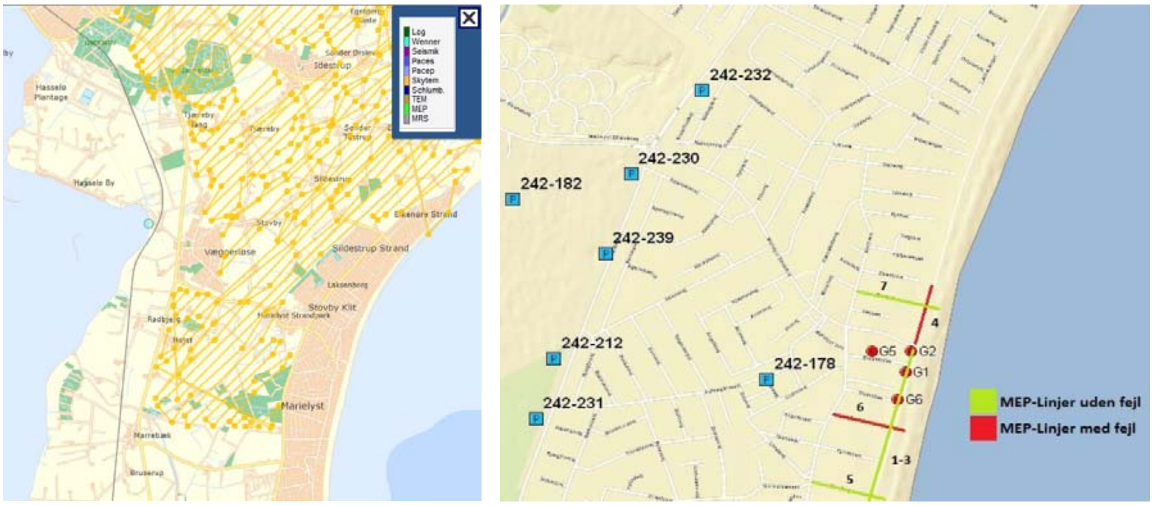

Figure 3-3. SkyTEM flight lines (left) and MEP profile lines (right)

SkyTEM surveys provide a good areal 3D coverage of resistivity measurements down to 100-150 meters below ground surface. The depth of investigation (DOI) varies depending of the vertical succession of layers and formation resistivities of these layers. The measured resistivities were inverted to both 5-layer models and 19 layer models. The conversion of SkyTEM resistivities to 3D lithological units for hydrogeological groundwater modelling is associated with uncertainties (He et al. 2014). The horizontal and vertical resolution of SkyTEM resistivity inversions depends among other things on the applied SkyTEM technology, the flight line density, and the sequence and properties of the local geology.

Five Multi Electrode Profiling (MEP) lines along and perpendicular to the eastern coastline, were collected in the area where it was not possible to use AEM methods (Figure 3-3). The MEP profiles give 2D resistivity information along the profile lines down to a depth of 60 meters (Steiness, 2011).

3.2.5 Data management and visualisation using GeoScene3D

The Danish software GeoScene3D (GS3D) is a software programme for visualizing, interpreting, editing and publishing geological data for e.g. groundwater modelling projects. In GS3D it is possible to visualize many different types of geological data, from for example boreholes, geophysics, terrain models, geological layers and water chemistry (http://i-gis.dk/).

SkyTEM resistivity profiles (flight lines) are interpolated with GS3D into grids values, which are converted to TDS values. Iso-resistivity maps and TDS values are interpolated and exported for later possible use in model calibration process.

3.3 Existing local groundwater model

3.3.1 Local model setup

As part of the BaltCICA project a variable density groundwater model was established for the study area to analyse possible effects of sea level rise, changed groundwater recharge and changed drainage stage on saltwater intrusion and groundwater quality (Rasmussen et al. 2013).

The numerical modelling complex MODFLOW-2000/MT3DMS/SEAWAT was used for simulating 3-D variable density groundwater flow and solute transport. Groundwater Vistas version 6 was used as the pre- and post-processing tool.

The Hydrogeologic-Unit Flow (HUF) Package for MODFLOW2000 was used to define hydrogeological units independently from the numerical layers. Hydraulic properties are assigned to the hydrogeological units in the HUF-package and the HUF-package calculates the effective hydraulic properties for the numerical layers of the flow model. The advantage of using the HUF-package is the ability to represent hydrological units of variable thickness and distribution independently of model layers in the flow model (Figure 3.4).

The model area is 44 km^2 of which 12 km^2 is sea. The horizontal grid size is 50 m by 50 m. The hydro-stratigraphical model implemented with the HUF-package has 15 geological layers, while the flow model consists of 32 numerical layers with thicknesses varying from 2 to 12 m. The thickness of the numerical layers gradually increases with depth down to −200 m a.s.l. A more detailed description of the model setup and climate scenarios is found in Rasmussen et al. (2013).

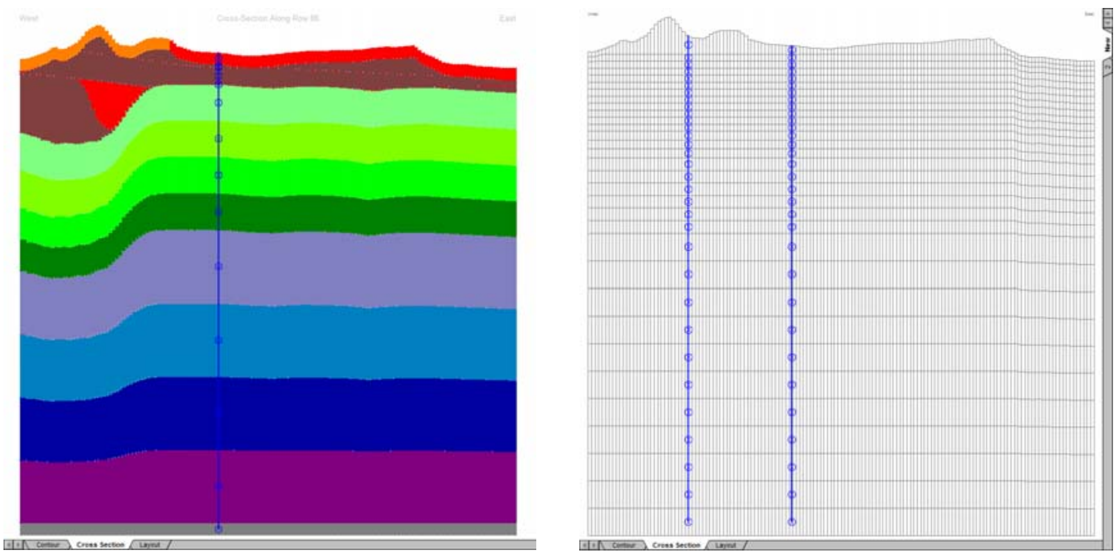

Figure 3-4. Cross section of the hydrogeological layering in the HUF-package setup (left) and the model layers in the groundwater flow model (right)

The hydraulic conductivities of the existing model are seen in Table 3-1, definition of hydraulic zones in Table 3-2, storage and porosity values in Table 3-3, and diffusion and dispersivity values in Table 3-4.

Table 3-1 Hydraulic conductivities of hydro-stratigraphical units (HUF-package). For explanation of blue and yellow colours, see Table 3-2 and text below Table 3-1

Layer	Lithology	Kx[m/d]	Kx[m/s]	Kz[m/d]	Kz[m/s]	Kz/Kx
1	fractured clay	0.43200	5.00E-06	0.04320	5.00E-07	0.1
1-6	sand	43.20000	5.00E-04	4.32000	5.00E-05	0.1
2-6	clayey till	0.08600	9.95E-07	0.00860	9.95E-08	0.1
7	chalk	4.32000	5.00E-05	0.43200	5.00E-06	0.1
8	chalk	0.86400	1.00E-05	0.08640	1.00E-06	0.1
9	chalk	0.43200	5.00E-06	0.04320	5.00E-07	0.1
10	chalk	0.08640	1.00E-06	0.02160	2.50E-07	0.25
11	chalk	0.00864	1.00E-07	0.00864	1.00E-07	1
12	chalk	0.00600	6.94E-08	0.00600	6.94E-08	1
13	chalk	0.00400	4.63E-08	0.00400	4.63E-08	1
14	chalk	0.00200	2.31E-08	0.00200	2.31E-08	1
15	chalk	0.00086	1.00E-08	0.00086	1.00E-08	1

The variations in hydraulic conductivities reflects the proposed zonation of salinity with depth from an advective zone in the upper part of the chalk formation, a transition zone below which the diffusion processes are dominating (Larsen et al. 2006; Bonnesen et al., 2009). The hydraulic conductivity of the drain bottom is 0.86 m/d.

Table 3-2 Hydraulic zones in the existing model

Hydraulic zones (chalk)	Zone thickness (m)	Layer (no.)	Hydraulic conductivity
Quaternary	5-35	1-6	K_{sand}, K_{clay}
Advective	15	7	K_A
Transition	30	8-9	$K_A \rightarrow K_T$
Diffusion	130	10-15	$K_T \rightarrow K_D$

Table 3-3 Storage and porosity values

Layer	Lithology	Ss (m^{-1})	Sy	Eff.Porosity
1	fractured clay	0.2	0.2	0.2
1	sand	0.25	0.25	0.25
2-6	sand	1.00E-04	0.2	0.2
2-6	clayey till	1.00E-04	0.05	0.05
7	chalk	1.00E-05	0.15	0.15
8-15	chalk	1,00E-05	0,35	0,35

Table 3-4 Diffusion and dispersivity values

Layer	Property	Value	Value
1-15	Diffusion	4.10E-05 (m^2/d)	4.75E-10 (m^2/s)
1-15	Dispersivity, Longit_D	8 (m)	
1-15	Dispersivity, Transv_D	0.05 (m)	
1-15	Dispersivity, Transv_V	0.001 (m)	

I order to minimize numerical dispersion a fine model discretization may be necessary. A rule of thumb is that the Peclet number should not be larger than 4. The Peclet number is the ratio between the length of the model grid cell and the longitudinal dispersivity. For models with higher Peclet number than 4, is has been recommend to use the TVD solver (Total Variation Diminishing) for the model simulations (Langevin et al. 2010). The grid size of the used flow and transport models are 50 m by 50 m.

The model simulations was divided into six phases with four separate but consecutive model setups and simulations with different boundary conditions to represent the historical changes in the area (Figure 3-5). The groundwater head and salinity distribution at the end of each model phase was used as initial heads and concentrations for the next model phase (Rasmussen et al., 2013).

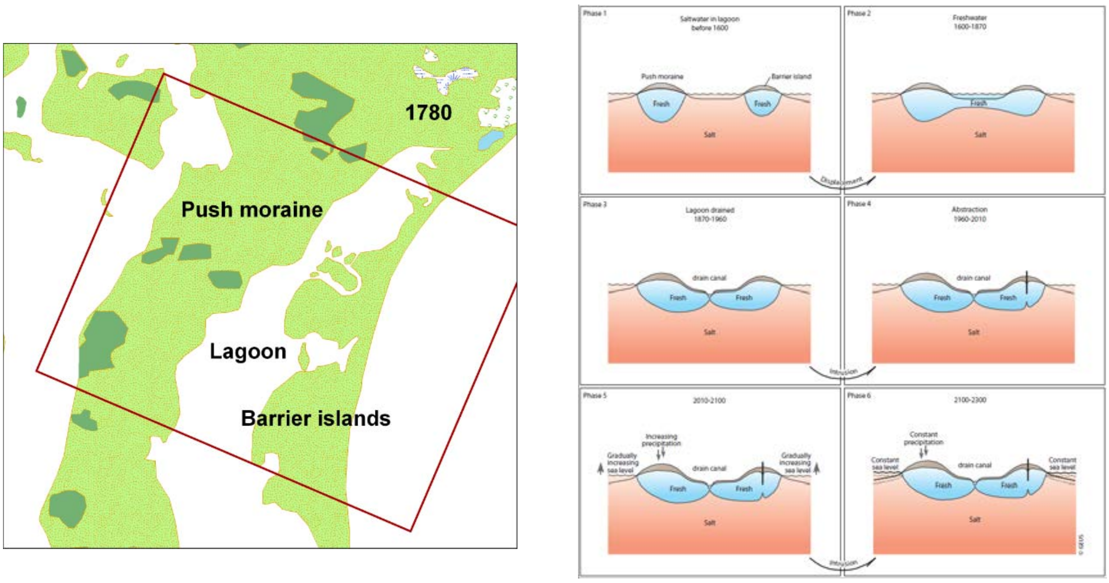

Figure 3-5. Landscape of study area around 1780 (left), and modelled transition phases of the area from a lagoon with barrier islands to reclaimed land with groundwater abstraction and climate change impacts (right), (Rasmussen et al., 2013)

The initial saltwater concentrations for modelling Phase 1 are seen in Figure 3-6.

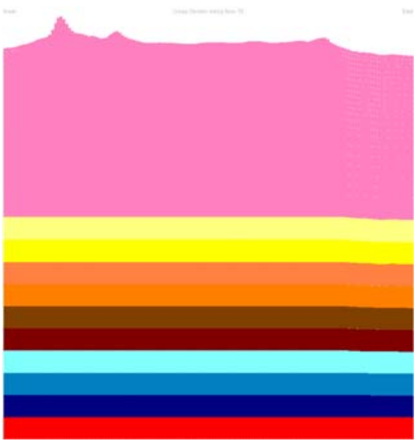

	Initial_C	Sorbed_C			Color
1	10	0	0	0	
2	10	0	0	0	
3	10	0	0	0	
4	10	0	0	0	
5	10	0	0	0	
6	12	0	0	0	
7	16	0	0	0	
8	20	0	0	0	
9	25	0	0	0	
10	30	0	0	0	
11	35	0	0	0	

Figure 3-6. The initial saltwater concentrations (Initial_C) for modelling Phase 1, model cross section (left), concentrations for each zone (the colours) in g TDS/l (right) from terrain to -200 m a.s.l.

3.3.2 Local model recalibration

Two methods are used to explore the possibilities of improving the calibration of the existing local groundwater model. The first method includes newly collected SkyTEM data and the borehole geophysics from the study area. The second method is a test of the pilot point method using groundwater heads.

Using geophysics

In the study area information from wireline logging in boreholes deep enough to show the upper part of the transition zone from the flushed advective zone with fresh water down towards the diffusion zone is only available from one well. The salinity gradient from this well is compared with logging results from other boreholes in chalk formations in the eastern Denmark.

The SkyTEM data have provided a good areal coverage of geological formation resistivities from large parts of the study area. Observed variations in the measured resistivities can be result of variations in either or both salinity and lithology. SkyTEM data can provide valuable information about depth to saltwater and the resistivity of geological formations. The accuracy of the SkyTEM measurements is not (so) high compared to wireline logging (GeofysikSamarbejdet, 2011). The SkyTEM measurements are limited to a certain depth, the "depth of investigations" (DOI) depending on the geology in the area, but usually it is between 100 and 200 meter below the ground surface.

A recalibration of the existing groundwater model where the detailed variations in geology and salinity obtained from the SkyTEM measurements are interpreted and used for model calibration lies outside the framework of this project. The approach using SkyTEM data for calibration will be to look at the possibility of interpolate an iso-resistivity surface corresponding to the upper boundary of the transition zone based on the corresponding resistivity and depth found with wireline borehole logging. This surface will define top of the specific model layer below which the transition zone is present and decreasing hydraulic conductivities are introduced in the layers below.

Using pilot points

The aim of using pilot points technique in the model calibration is to explore the effects of (small scale) geological variability. The distribution of hydraulic conductivity within the model domain or a geological unit can be described by a set of pilot points. Individual pilot points can be assigned to different hydraulic conductivity zones/geological units/model layers within the model domain. Only those points assigned to a particular zone or geological unit can be used in calculating hydraulic conductivities values throughout that zone using the kriging interpolation procedure. The variogram upon which kriging is based can be different in each zone, reflecting differences in the geology, or in the level of heterogeneity, expected within each geological unit. The parameter estimation software PEST is used to estimate the hydraulic conductivity of the zone/aquifer at each such pilot point. These point hydraulic conductivities will then be spatially interpolated to all of the active cells within the model domain using kriging (Rumbaugh, 2013).

In the study area the main part of the groundwater head observations are from the upper 10-20 meters of the chalk. The model layer containing the most head observations are chosen for the pilot point calibration, for other layers the manual calibration procedure is used.

A number of pilot points are introduced to the model layer 7, where most groundwater head observations are found (Figure 3-8). Each pilot point is defined by a number, xy coordinates, layer number, hydraulic conductivity target value Kx (Kz), minimum Kx (Kz), and maximum Kx (Kz). The location of pilot points are subjective, but conventional wisdom tells that the number of parameters involved in a parameter estimation should be kept to a minimum. Using pilot points in conjunction with PEST's regularization functionality prevents the onset of numerical instability. The regularization brings a high degree of numerical stability to a parameter estimation problem if regularization constraints are appropriately defined. The pilot point procedure includes a calibration constraint “homogeneous unless proven otherwise”, so heterogeneity is only introduced in the calibration process “because it has to be there”. A set of “kriging factors” for each of the cells of the finite difference grid can be calculated by Groundwater Vistas in advance of the actual interpolation process (Rumbaugh, 2013).

Rule of thumb for pilot point calibration (Rumbaugh, 2013):

- The number of pilot points should be 2 – 3 times the numbers of observations (targets)
    - For horizontal Kx use target triangulation for location of pilot points and afterwards fill the gaps with pilot points
    - For vertical Kz place pilot points at target locations and afterwards fill the gaps
- Combine ‘truncated SVD’ and ‘SVD assist’
- Use ‘super pilot points’. The number of super pilot points should be 10 – 20 % of the number of pilot points
- Use ‘preferred homogeneity’
- If there are no observations in a zone PEST will not be able to do a good estimate of the parameters
- Variogram: α could be 20 % of the maximum dimension of the zone
- Kriging search radius: large enough so that every cell within the zone can have an interpolated value.

The pilot point calibration is performed as a non-variable (uniform) density modelling. Areas with high salinity in the existing local model are converted to no-flow cells (Figure 3-9).

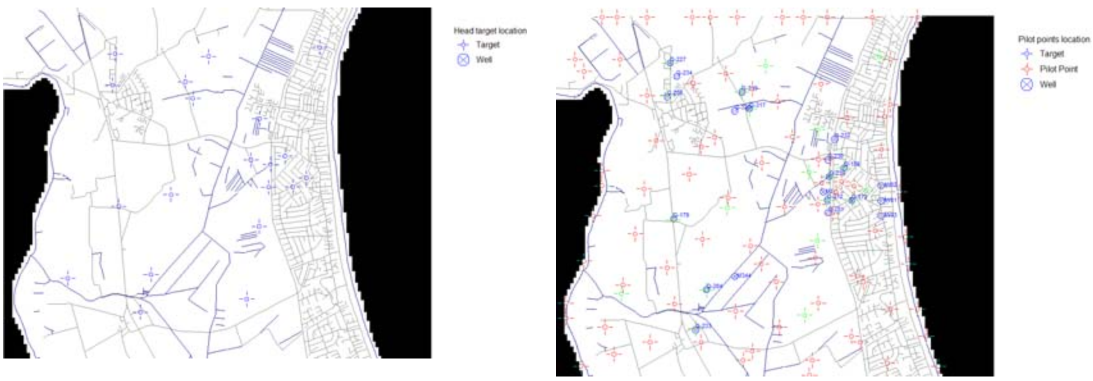

Figure 3-7. Groundwater head observations in model layer 7 (left). Location of pilot points, Kx red cross, Kz green cross (right)

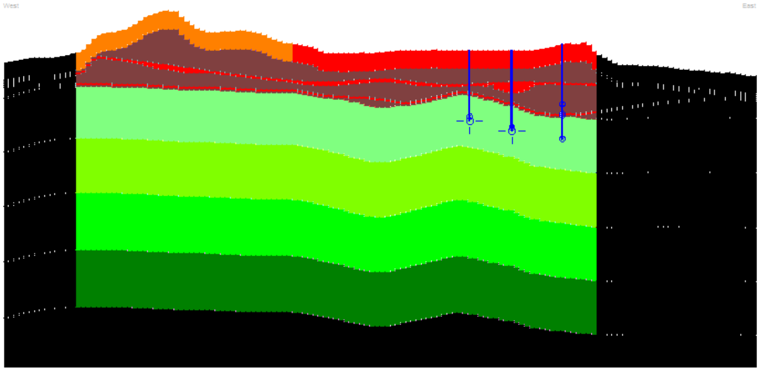

Figure 3-8. Areas with high salinity in existing model are converted to no-flow cells (black) for the pilot point tests

3.3.3 Injection well setup

Four out of a number of suggested possible scenarios of injection well designs and pumping rates were analysed with the variable density groundwater model (Table 3-7).

Table 3-5 Injection wells scenarios, the ones marked with yellow were completed

Injection scenario	Number of wells	Well Direction[1,5]	Pumping schedule[2,3]	Pumping rate (%)	Model recalibration	Climate scenario[4]
1	3	Vertical	Constant	100	Before	3
2b	3	Vertical	Constant	100	After	3
2e	3	Vertical	Constant	100	After	2
	2	Vertical	Constant	100	After	
	2	Vertical	Recirculating	100	After	
	2	Vertical	Recirculating	50	After	
	3	Vertical	Alternating	50/0	After	
2c	3	Vertical	Alternating	100/0	After	3
	3	Vertical	Constant	50	After	
	3	Vertical	Constant	200	After	
2d	1	Horizontal	Constant	100	After	3
	1	Horizontal	Constant	50	After	
	1	Horizontal	Alternating	100/0	After	

1. Wells placed parallel to coastline, except recirculation wells
2. Recirculation of groundwater between one pumping and one injection well (ATES system) perpendicular to coastline
3. Alternating pumping schedule: half year pumping / half year pause
4. Scenario 3: Sea level rise +0.75 m and decrease in groundwater recharge by 15%. Scenario 2: Sea level rise +0.75 m and no change in groundwater recharge (Rasmussen et al., 2013)
5. Length of horizontal well: 150 m (length of three model cells).

The three synthetic injection wells are located 300 m from the coast with 250 m spacing. An injection rate equal to the average abstraction rate from each of the waterworks abstraction wells, 68 m^3/d (24,820 m^3/y), is used as point of reference (100%). The well screens are placed in the upper fractured chalk -12 to -30 m a.s.l. (meter above sea level). An alternating pumping schedule is applied in one scenario: ½ year pumping and ½ year pause (Figure 3-9).

For the horizontal well a screen length of 150 m is used, which is the length of three model grid cells. The horizontal well is located -18 to -21 m a.s.l. and 300 m from the coast line. The horizontal well is implemented in MODFLOW in as a standard boundary condition (Figure 3-9).

Year 2300 marks the end of the test of the climate change scenarios in the existing model, therefore the injection of water with the injections wells is started in year 2300 and the simulation is continued for additional 100 years (Rasmussen et al. 2013).

Figure 3-9. Location of injection wells, plan view left, cross section right. Vertical injection wells (upper) and horizontal well (lower)

3.3.4 Climate change scenarios

In the existing model eight climate change scenarios were simulated with different combinations of sea level rise, groundwater recharge, and drainage canal stage. Scenario 0 represents a situation where no changes occur. Scenario 1 represents an estimate of the most likely future with an increase in recharge of 15% and sea level rise of 0.75 m. In scenario 2–8 a sensitivity analysis of the most likely scenario is carried out, where other realistic changes in sea level and recharge have been implemented. The drainage canals play an important role in the modelled groundwater system. To evaluate the sensitivity of the drains, two simulations (scenarios 7 and 8) are performed with changed stage, +30 and −30 cm, respectively (Rasmussen et al. 2013).

For the present study two climate change scenarios were selected: Scenario 3: Sea level rise +0.75 m and decrease in groundwater recharge by 15%, and Scenario 2: Sea level rise +0.75 m and no change in groundwater recharge (Table 3-5).

3.4 Generic groundwater models

3.4.1 Model setup

The generic models are simplified model setup of the existing groundwater model for the Marielyst area. Similar model boundary conditions and parameters are to some extent used as a starting point for the generic models. But the generic model area is smaller, the geological model is simpler, and the generic models consist of fewer calculation layers (Table 3-6, 3-7, 3-8, 3-9, 3-10, and Figure 3-10).

Table 3-6. Basic data for setup of generic models

Model setup	Value	Unit
rows	40	
columns	40	
layers	12	
grid x	50	m
grid y	50	m
top elevation.	10	m
bottom elevation	-70	m
layer average thickness	6.67	m
total active cells	192,000	
total area	4,000.000	m2
Stress periods		
SP-1	36,500	d
SP-2	328,500	d
No. time steps		
SP-1	10	
SP-2	100	

Table 3-7. Hydraulic conductivities of the standard generic model

Layer	Lithology	Kx[m/d]	Kx[m/s]	Kz[m/d]	Kz[m/s]	Kz/Kx
1-2	sand	43.2	5.00E-04	4.32	5.00E-05	0.1
3	clayey till	0.0864	1.00E-06	0.00864	1.00E-07	0.1
4-7	chalk1	4.32	5.00E-05	0.432	5.00E-06	0.1
8-11	chalk2	4.32	5.00E-05	0.432	5.00E-06	0.1
12	chalk3	0.000864	1.00E-08	0.000864	1.00E-08	1

Table 3-8. Storage and porosity values for the standard generic model

Layer	Lithology	Ss (m-1)	Sy	Effective Porosity
1-2	sand	0.25	0.25	0.25
3	clayey till	1.00E-04	0.05	0.05
4-7	chalk1	1.00E-05	0.15	0.15
8-11	chalk2	1.00E-05	0.15	0.15
12	chalk3	1.00E-05	0.35	0.35

Table 3-9. Diffusion and dispersivity values for the standard generic model

Layer	Property	Value	Value
1-12	Diffusion	4.10E-05 (m^2/d)	4.75E-10 (m^2/s)
1-13	Dispersivity, Longit_D	8 (m)	
1-14	Dispersivity, Transv_D	0,05 (m)	
1-15	Dispersivity, Transv_V	0,001 (m)	

Table 3-10. Boundary conditions for generic models

Boundary conditions		Value	Unit	Note
Recharge				
		0.0007	m/d	
		0.00081	m/d	climate scenario +15%
	concentration	0.5	g TDS/l	
Pumping, 1 well: P1				
	SP-1	0		
	SP-2	68	m3/d	model layer 5
Drain				
	Stage of drain	-1	m	
	Width of drain	2	m	
	Length of drain in cell	50	m	
	Thickness drain bed	0.5	m	
	Hydraulic conductivity	0.172	m/d	
	Conductance	34.4	m2/d	
Fixed Head				
		0	m	
		+0.5	m	sea lever rise
Sea concentration				
		10.5	g TDS/l	
Bottom layer concentration				
		10.5	g TDS/l	

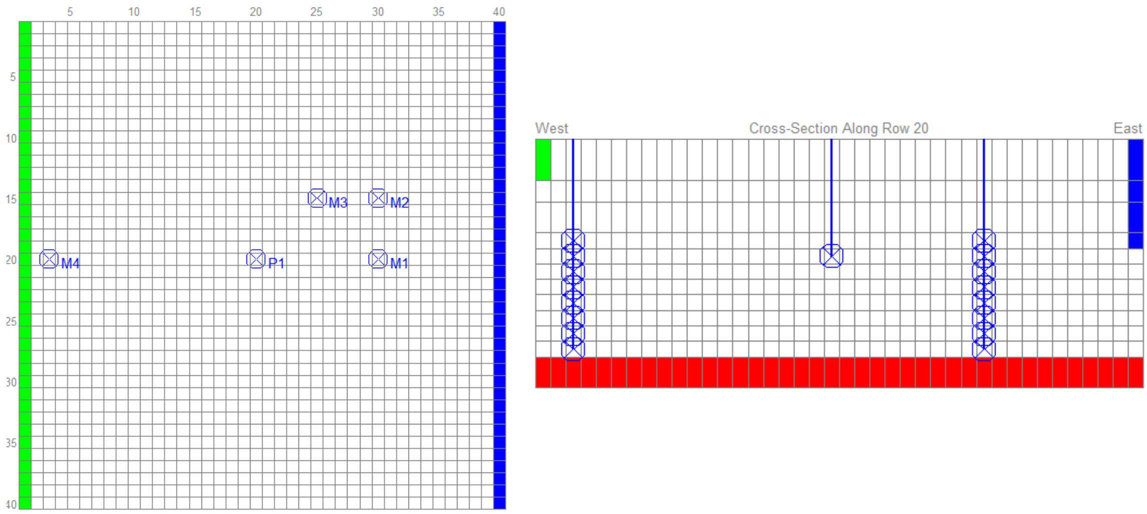

Figure 3-10. Horizontal (left) and vertical (right) view of standard generic model. P1 is the pumping well, M1-M4 are monitoring wells

3.4.2 Sensitivity analysis

The generic models are used to test and compare the effect of changes in different model boundary conditions (BC) and parameters like bottom layer concentrations, diffusion coefficients and hydraulic conductivity of aquitard. Scenarios 1-4 are generic models including saltwater diffusion only, where all other scenarios include saltwater intrusion (Table 3-11).

Table 3-11. Scenarios with generic models (BC: boundary condition 1-4, H: Head, C: concentration, avg.: average value, Q: pumping rate, SWI: saltwater intrusion)

Sce. no	Chalk model	BC1	BC2	BC3	BC4	Diff. coef	Aquit. Kx,z	Rech	Remarks
1	2 layer	Const.H	Q avg.	Const.C		avg.	avg.	avg.	Diffusion only
2	2 layer					high			
3	2 layer						low		
4	2 layer			C high					
5	2 layer	Drain	Q avg.	Const.C	Const. H.C.4layers	avg.	avg.	avg.	SWI and canal
6	2 layer				Const. H.C.3lyers				
7	3 layer				Const. H.C.4layers				K1 > K2 > K3,
8	3 layer		Q high						
9	2 layer				+1.0m				SLR 1.0 m
9b	2 layer				+0.5m				SLR 0.5 m
10	2 layer							+15%	Recharge Increase 15%
11	2 layer						low		

In scenario 6 the seawater intrusion boundary condition with constant head and concentration is assigned to layer 1-3, whereas in other scenarios the same boundary condition is assigned to layer 1-4.

In scenarios 8-10 the effect of projected climate change are illustrated by modelling sea level rise and changed groundwater recharge.

3.4.3 Hydraulic barrier setup

Five scenarios with injection of water into the aquifer with the purpose of creating a hydraulic barrier to protect the groundwater abstraction wells from saltwater is analysed with the generic models. The scenarios focus on injection rates and well configurations, numbers of wells, vertical or horizontal wells (Table 3-12 and Figure 3-11).

Table 3-12. Injection wells scenarios with generic models (BC: boundary condition 1-4, H: Head, C: concentration, avg.: average value, Q: pumping rate)

Sce. no	Chalk model	BC1	BC2	BC3	BC4	Inject. well	Remarks
12	2 layer	Drain	Q avg.	Const.C	Const. H.C.4layer	1 vert.	Q = 68 m3/d Qconc.= 0 g/l
12b	2 layer		Q avg.			1 vert.	Q = 68 m3/d Qconc.= 0,5 g/l
13	2 layer		1/4 Q avg.			1 vert.	Q = 17 m3/d
14	2 layer		Q avg.			3 vert.	Q = 22.7 m3/d for each well
15	2 layer		1/4 Q avg.			1 horiz.	1 layer, length: 3 cells = 150 m

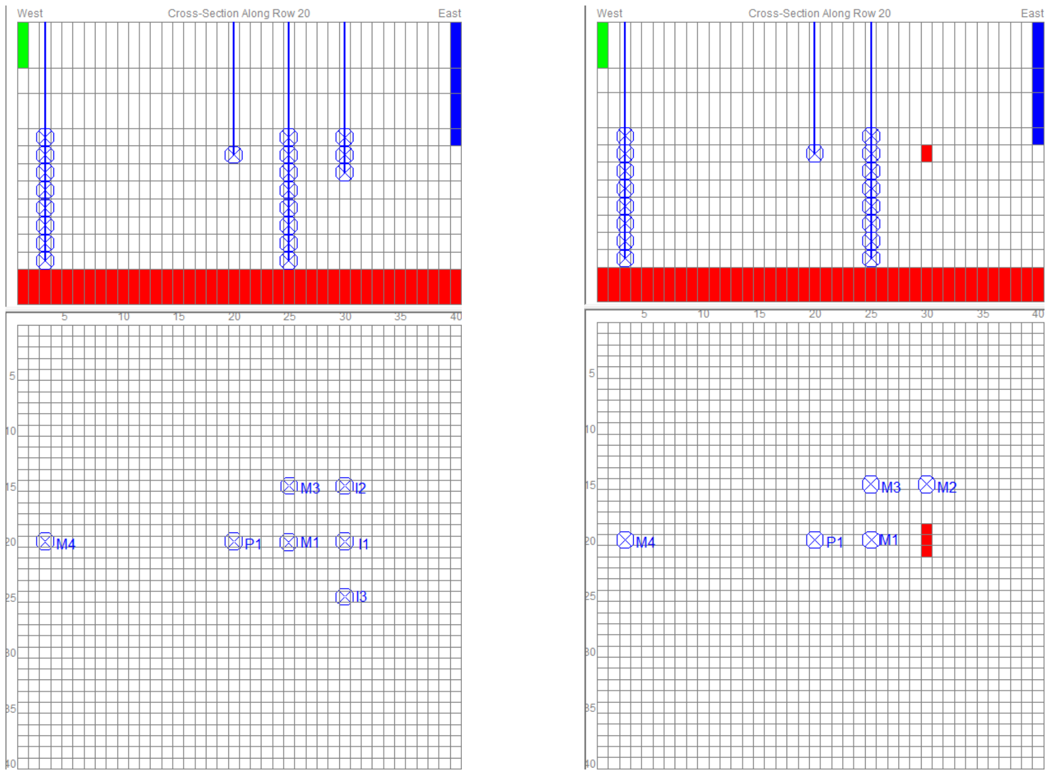

Figure 3-11. Generic model setup for scenario 14 with 3 injection wells (left) and scenario 15 with 1 horizontal well (right). P1 pumping well, M1-M4 monitoring wells

3.4.4 Monitoring system designs

Depending on the generic model setup 3-4 monitoring wells are placed between the pumping well and the coast, between the pumping well and the injection well, and near the canal. The monitoring wells have a monitoring point in each model layer in the chalk aquifer (Figure 3-10 and 3-11).

4. Results

4.1 Sources of salinity

If the molar ratio of sodium to chloride [Na]/[Cl] is below 0.9 the salinization is most likely to come from seawater intrusion. If the ratio is above 0.9 diffusion of connate saline water is the most like source of chloride. Data from the deeper groundwater abstraction wells in the area, marked with light green in Table 4-1, all have a ratio below 0.9, with an average ratio of 0.8.

Table 4-1. Groundwater [Na]/[Cl] ratio

Borehole	Depth (mbgs)	Date	Na[mg/l]	Na[mmol/l]	Cl[mg/l]	Cl[mmol/l]	Na/Cl
242.44B	17,00	10-04-1970	74,00	3,22	148,00	4,17	0,77
		26-06-1989	130,00	5,65	228,00	6,43	0,88
		15-01-2004	143,00	6,22	293,00	8,27	0,75
242.178	23,00	10-04-1970	30,00	1,30	53,00	1,50	0,87
		26-06-1989	110,00	4,78	202,00	5,70	0,84
		29-01-1996	135,00	5,87	255,00	7,19	0,82
		24-01-2013	130,00	5,65	270,00	7,62	0,74
242.172	18,50	26-06-1989	47,00	2,04	101,00	2,85	0,72
		23-01-2015	110,00	4,78	208,00	5,87	0,82
242.190	19,00	10-04-1970	29,00	1,26	50,00	1,41	0,89
		12-06-1995	128,00	5,57	270,00	7,62	0,73
		21-01-2003	109,00	4,74	262,00	7,39	0,64
242.212	15,60	26-06-1989	55,00	2,39	113,00	3,19	0,75
		07-01-2013	88,00	3,83	200,00	5,64	0,68
242.230	15,00	26-06-1989	29,00	1,26	57,00	1,61	0,78
		23-01-2015	58,00	2,52	120,00	3,39	0,75
242.232	17,00	26-06-1989	60,00	2,61	118,00	3,33	0,78
		23-01-2015	86,00	3,74	162,00	4,57	0,82
242.317	13,00	11-01-2006	16,00	0,70	35,00	0,99	0,70
		23-01-2015	23,00	1,00	36,00	1,02	0,99
242.319	16,00	26-05-2005	17,00	0,74	29,00	0,82	0,90
		16-01-2012	21,00	0,91	41,00	1,16	0,79
242.320	14,00	26-05-2005	21,00	0,91	37,00	1,04	0,88
		24-01-2013	17,00	0,74	31,00	0,87	0,85

There is a tendency to decreasing values of the [Na]/[Cl] ratio as the sodium and chloride concentration increase, which indicate that sea water intrusion is taking place.

4.2 Geophysics and saltwater distribution

Wireline logging from the 100 m deep borehole in the study area has provided data indicating that the advective zone is deeper than assumed in the old model setup, approximately 20 m (Figure 4-1).

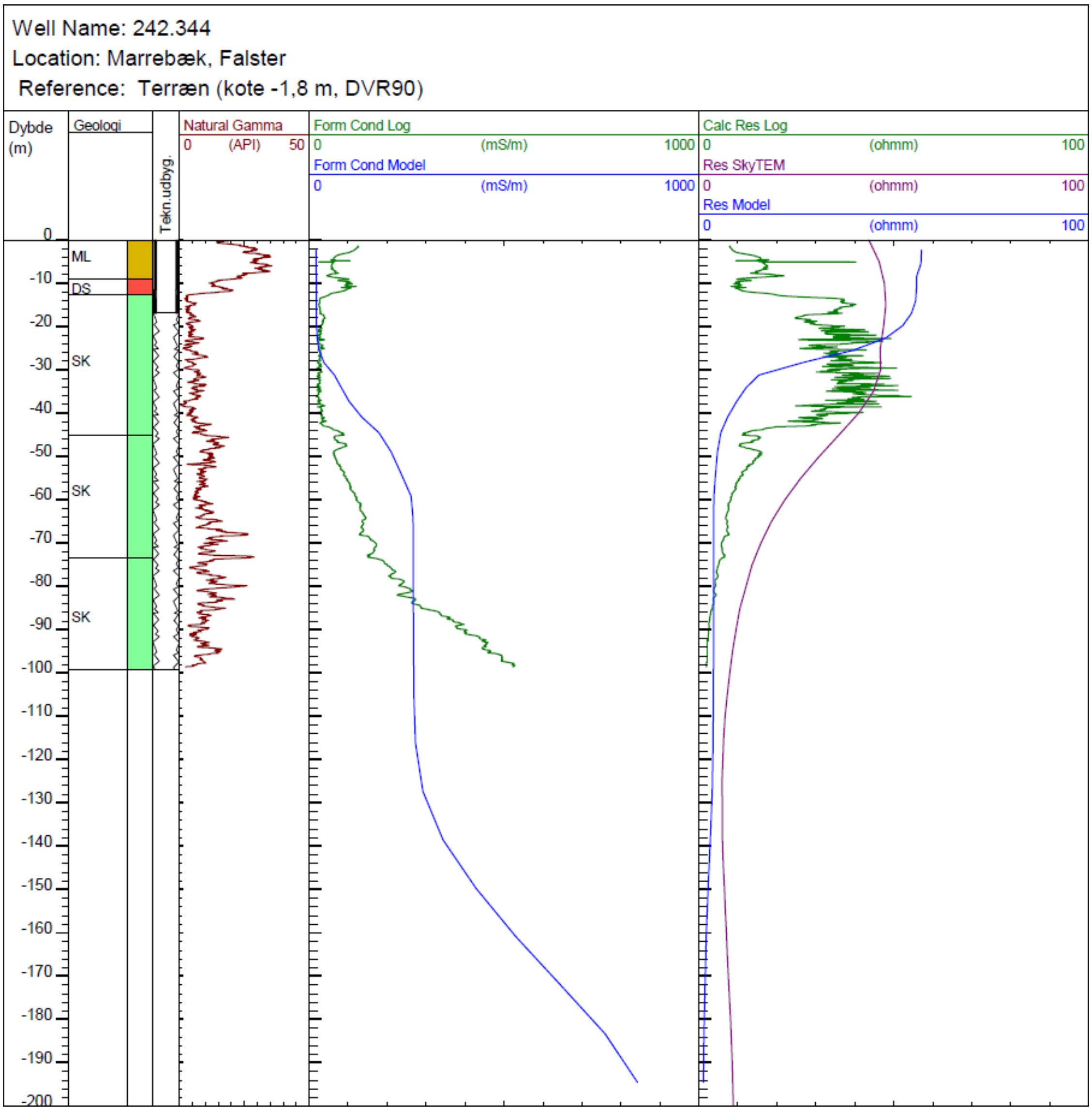

Figure 4-1. Centre column showing formation conductivity from wireline logging (green) and modelled formation conductivity calculated from TDS concentrations (blue). Right column shows the formation resistivities including the SkyTEM measurements (magenta). The left column shows the natural gamma radiation

In the study area there is only information from wireline logging from one borehole that is deep enough to capture the upper part of the transition zone from the flushed advective zone with fresh water down through the upper part of the transition zone. The salinity gradient from this well is in good accordance with logging results from other boreholes in chalk formations in the eastern part of Denmark (Figure 4-2). This salinity gradient is to some extent modelled and reproduced with the existing model using a gradually decreasing hydraulic conductivity with depth in the transition zone and appropriate initial conditions (Section 3.3.1.).

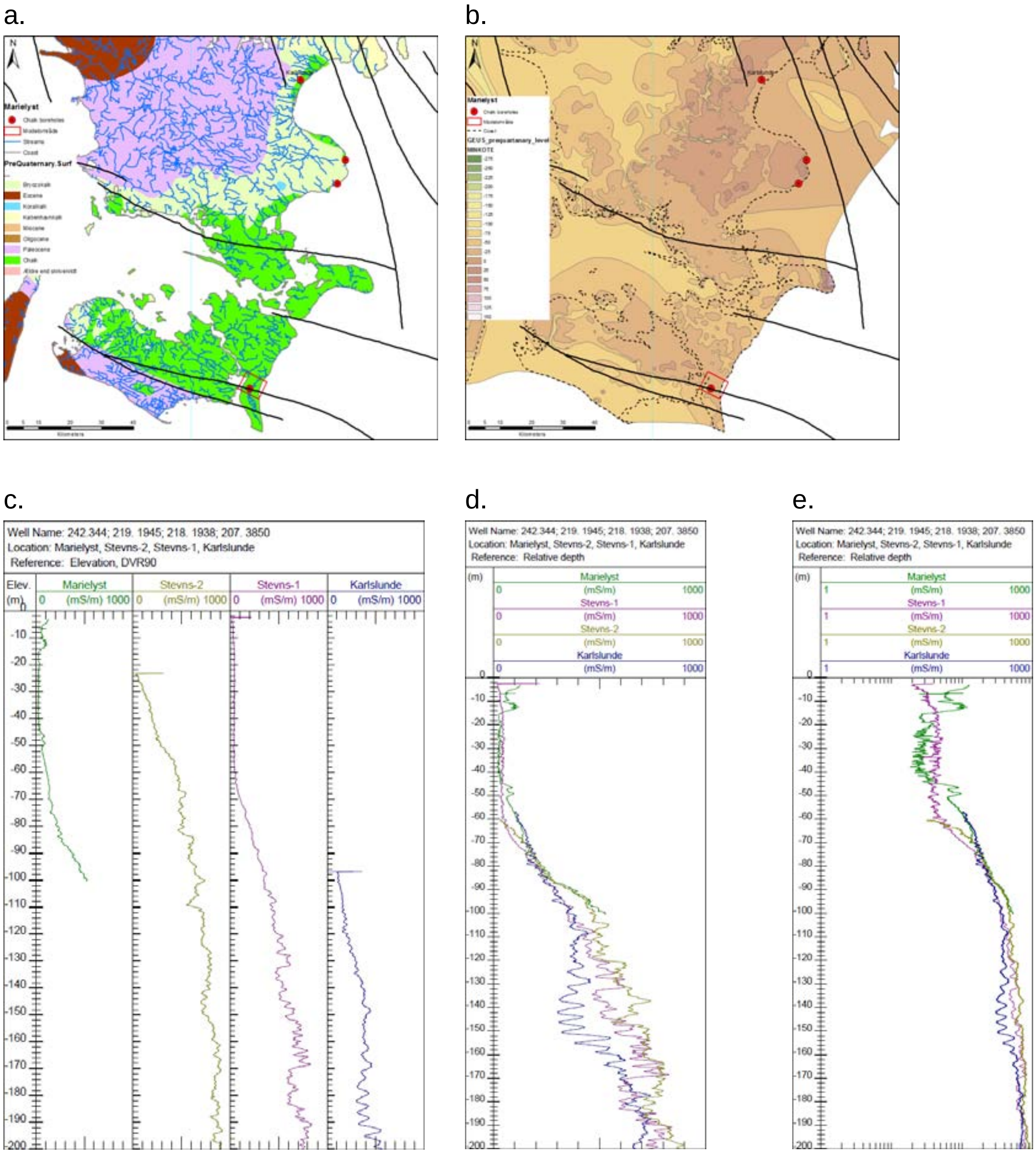

Figure 4-2. a. Location of deeper research boreholes in chalk and top pre-quaternary geology, b. Location of deeper research boreholes in chalk and top pre-quaternary elevation, c. Formation conductivity from wireline logging of the four boreholes, left to right corresponds to south to north location of boreholes in panel a. and b., d. The four induction logs depth shifted to match similar gradients, normal scale, e. The four induction logs depth shifted to match similar gradients, log scale

It is observed that the gradient (the increase of formations conductivity with depth) is of the same magnitude when comparing the deeper borehole in the study area with other boreholes in chalk settings in the eastern part of Denmark. In Figure 4-2 a comparison of wireline induction logs from four chalk boreholes in eastern Denmark (Study area Marielyst, Stevns-2, Stevns-1, and Karlslunde, order of well names correspond to south to north location on maps).

Even though the elevation where the transition from advective dominated zone to the diffusion dominated zone varies from location to location, the logging results indicate that the proposed conceptual model with a well-defined advective zone above a well-defined transition zone can be generalised to the chalk aquifer in the study area. The salinity gradients from Marielyst and Karlslunde are very similar, and the gradients from Stevns-2 and Stevns-1 are very similar.

With SkyTEM measurements a good areal coverage of geological formation resistivities has been obtained from large parts of the study area (Figure 4-3).

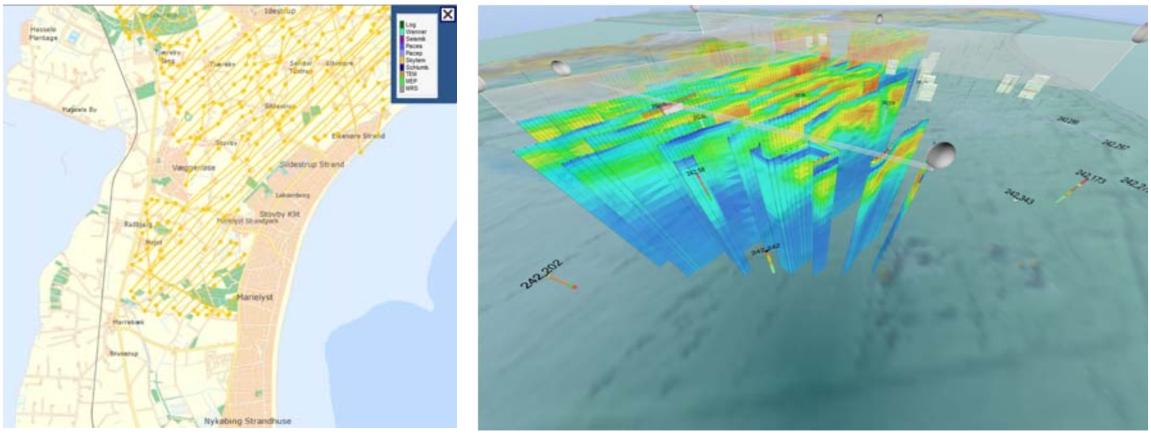

Figure 4-3. SkyTEM flight lines (left). SkyTEM resistivities displayed in 3D (right)

Observed variations in the measured resistivities can be result of variations in either or both salinity and lithology. SkyTEM data can provide valuable information about depth to saltwater and the resistivity of geological formations. The accuracy of the AEM measurements is not (so) high compared to e.g. wireline logging (GeofysikSamarbejdet, 2011). The SkyTEM measurements are limited to a certain depth, the “depth of investigations” (DOI) depending on the geology in the area, but usually between 60 and 120 meter below the ground surface (Figure 4-4).

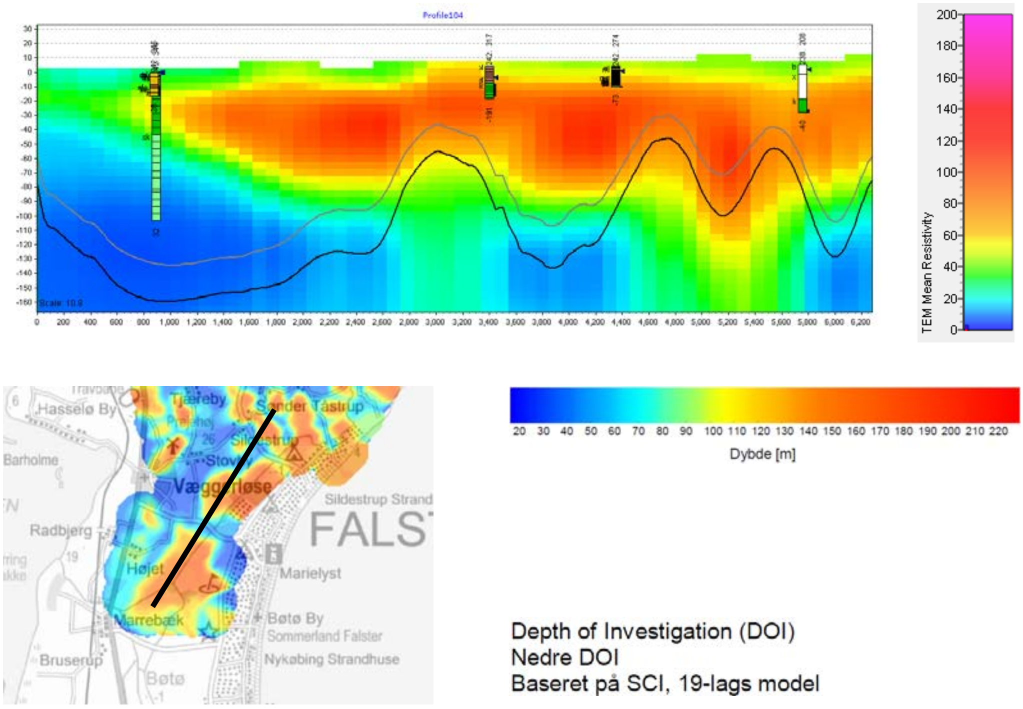

Figure 4-4. Cross section showing the upper (grey) and lower (black) Depth Of Investigation (DOI), and SkyTEM resistivities (upper panel). Map showing lower DOI and location of cross section (lower panel)

A recalibration of the existing groundwater model where the detailed variations in geology and salinity obtained from the SkyTEM measurements are interpreted and used for model calibration lies outside the framework of this project. The original idea was to interpolate an iso-resistivity surface corresponding to the upper boundary of the transition zone based on the corresponding resistivity and depth found with wireline borehole logging. This surface would define the top of the specific model layer below which the transition zone is present and decreasing hydraulic conductivities are introduced in the layers below.

As described above the SkyTEM survey did not cover the entire model area, so it is not possible to use the SkyTEM data to define the bottom of the advective zone for the whole model area. Figure 4-4 shows how the transition zone extends deeper north of the borehole (242.344), from about -60 m at the borehole to -100 m around 1000 m north of the borehole where it levels out. The grey line in fig Figure 4-4 shows the upper DOI (Depth Of Investigation) and the black line the lower DOI. In areas where the SkyTEM data shows deeper zones of higher resistivities the DOI is at higher elevations in most but not all cases. In general the DOI varies between -60 m to -160 m a.s.l., with an average investigation depth of -100 to -120 m a.s.l.

Figure 4-5 shows SkyTEM resistivities for different 10 m depth intervals. In the central part of the area a west-east section is seen with lower resistivities compared to the surrounding areas. This area coincides with an area where saltwater is located deeper based on TEM soundings (Storstrøms Amt, 2000).

a.
Resistivities: -40 - -50 m

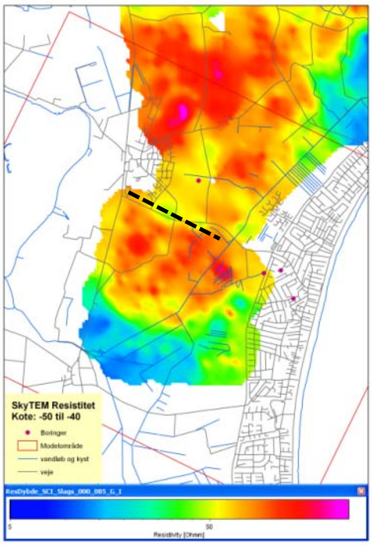

b.
Resistivities: -80 - -90 m

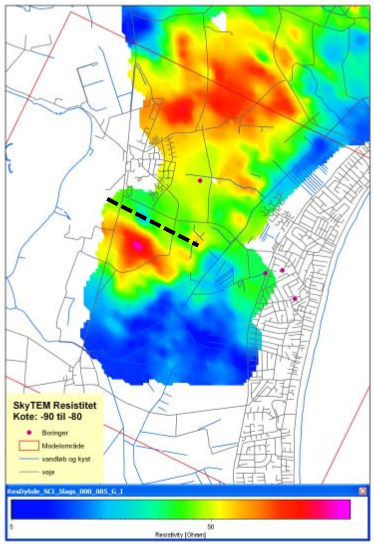

c.
Resistivities: - 120- -130m

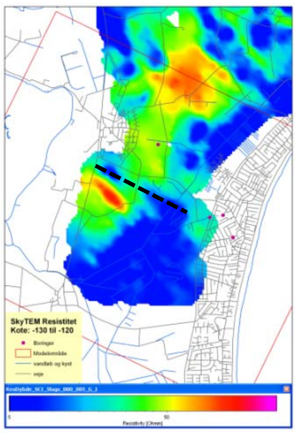

d.
Depth to saltwater

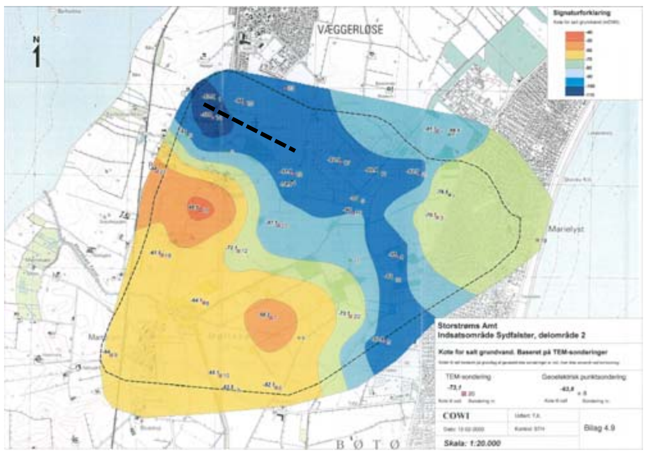

Figure 4-5. a., b., c. show SkyTEM for different 10 m depth intervals and d. is depth to saltwater based on TEM soundings (Storstrøms Amt, 2000). Black dotted line showing area with low resistivities and high depth to saltwater compared to surrounding areas

Figure 4-6 shows a combined plot of formation conductivity from wireline logging and SkyTEM resistivities, a good overall agreement in the changes with depth of the conductivity/resistivity is seen.

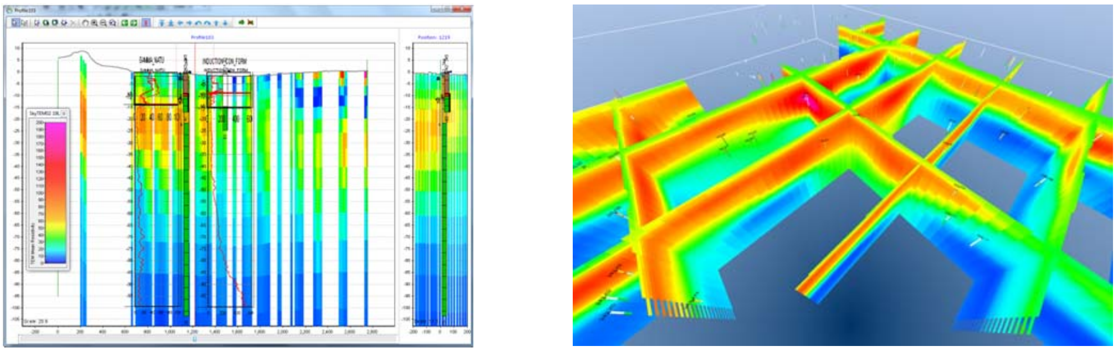

Figure 4-6. Combined plot of formation conductivity from wireline logging and SkyTEM resistivities (left), and example of 3D-interploation of SkyTEM resistivities (right)

With GeoScene3D it is possible to make a 3D-interploation of SkyTEM resistivities (Figure 4-6). With the 3D-grid of SkyTEM resistivities it is possible to draw 3D interpolated iso-surface of e.g. 20 ohm-m resistivity and compare it with the DOI (Figure 4-7).

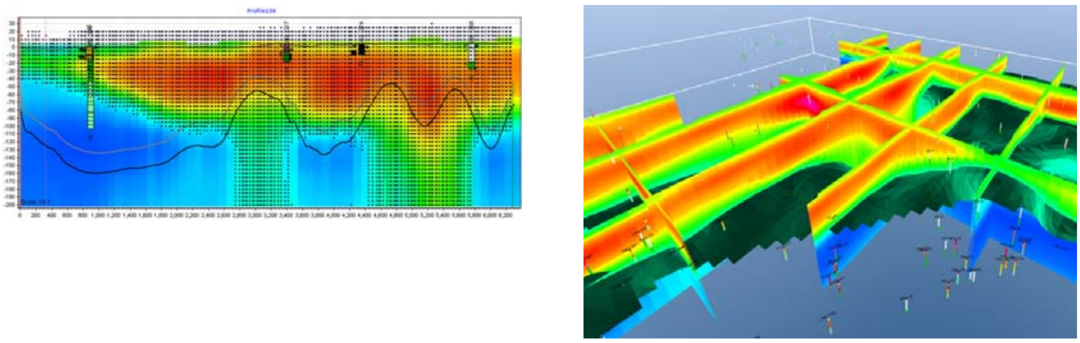

Figure 4-7. Combined plot of upper (grey) and lower (black) SkyTEM DOI and SkyTEM resistivities greater than 20 ohm-m (black dots) (left), and 3D interpolated iso-surface of 20 ohm-m resistivity (right)

The DOI (upper and lower) limits in certain areas the possibility to use SkyTEM data to estimate the areal distribution of the depth to the bottom of the advective zone, the top of the transition zone. The variations in the location of the DOI are related to the succession of soil resistivities.

Due to the partial coverage of SkyTEM data and the limitations from the SkyTEM DOI it was decided to limit the changes in the model setup for the recalibration to a change in the hydraulic conductivities for the advective zone base on the borehole wire-line logging and keep the elevation of the different conductivity zones as they are, it means keep the model layers as they were in the old model.

The results of MEP soundings in eastern part of the built-up area around the waterworks oldest well field indicates the existence of layers of mud and peat with higher formation conductivity (wireline logging data) and low formations resistivity (MEP soundings) between 5 to 9 meters depth compared to the clayey layers 9 – 15 m depth, top of chalk (Figure 4-8,

Appendix 3) (Steiness, 2011). The mud and peat layers may contain trapped interglacial/post glacial saltwater as the conductivity is higher than seen in the clay layers.

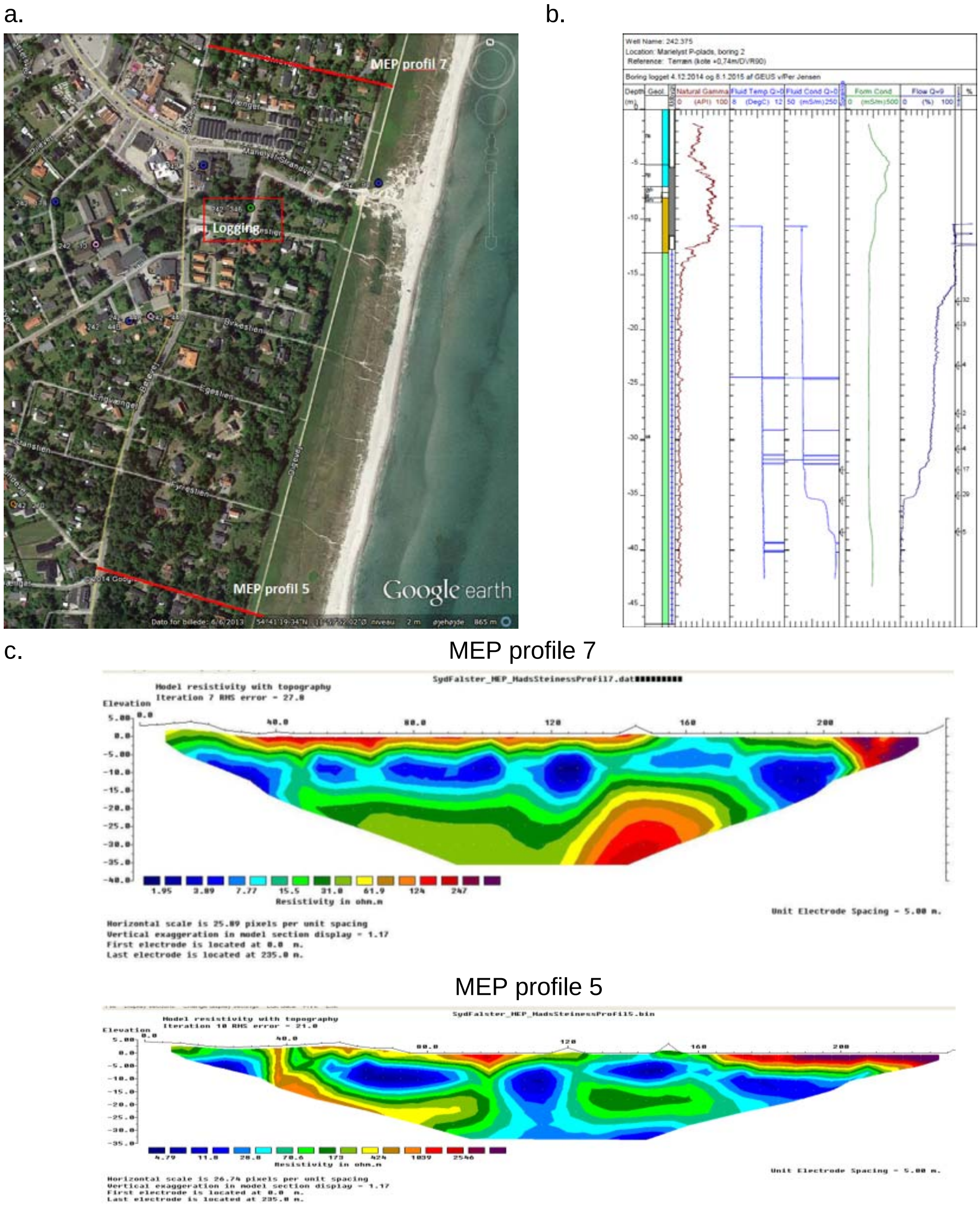

Figure 4-8. a. Location of borehole for wireline logging and MEP profile 5 and 7, b. wireline logging new borehole (242.375), c. MEP resistivity profiles no. 7 and 5

4.3 Recalibration of existing local model

4.3.1 Using geophysics

Based on the borehole geophysics the hydraulic conductivities of the hydro-stratigraphical model (HUF-model) layer 9 were increased to the same parameter values as layer 8 in order to increase the advective zone. To maintain a gradual decrease of hydraulic conductivities with depth all K-values were moved one layer up compared to the old model from layer 9 down to layer 14 (HUF model). The transition zone is now mainly HUF-model layer 9 and 10 (Table 4-2, 4-3, and 4-5).

Table 4-2. Hydraulic zones in the new adjusted model

Hydraulic zones (chalk)	Zone thickness	Layer	Hydraulic conductivity
Quaternary	5-35	1-6	K_{sand}, K_{clay}
Advective	30	7-8	K_A
Transition	30	9-10	$K_{A \to} K_T$
Diffusion	120	11-15	K_D

Table 4-3. Hydraulic conductivities in the new adjusted model (HUF-model)

Layer	Lithology	Kx[m/d]	Kx[m/s]	Kz[m/d]	Kz[m/s]	Kz/Kx
1	fractured clay	0.43200	5.00E-06	0.04320	5.00E-07	0.1
1-6	sand	43.20000	5.00E-04	4.32000	5.00E-05	0.1
2-6	clayey till	0.08600	9.95E-07	0.00860	9.95E-08	0.1
7	chalk	4.32000	5.00E-05	0.43200	5.00E-06	0.1
8	chalk	4.32000	5.00E-05	0.43200	5.00E-06	0.1
9	chalk	0.86400	1.00E-05	0.08640	1.00E-06	0.1
10	chalk	0.43200	5.00E-06	0.04320	5.00E-07	0.1
11	chalk	0.08640	1.00E-06	0.02160	2.50E-07	0.25
12	chalk	0.00864	1.00E-07	0.00864	1.00E-07	1
13	chalk	0.00600	6.94E-08	0.00600	6.94E-08	1
14	chalk	0.00400	4.63E-08	0.00400	4.63E-08	1
15	chalk	0.00200	2.31E-08	0.00200	2.31E-08	1

The variations in hydraulic conductivities reflects the proposed zonation of salinity with depth from an advective zone in the upper part of the chalk formation, a transition zone below which the diffusion processes are dominating (Larsen et al. 2006; Bonnesen et al., 2009).

The gradual change (with depth) in hydraulic conductivities from layer to layer follows the recommendations for making the variable density modelling process more smooth.

The initial concentrations in the new model setup were adjusted according to measurements from wire line logging of the formation electrical conductivity (Table 4-4).

Table 4-4. Initial concentrations in old and new adjusted model (Flow-model)

Flow model Layer	ConcZone	TopLayer	BotLayer	InitC-new	InitC-old
1-22	1	10	-90	10,000	10,000
23	2	-90	-101	12,000	10,000
24	3	-101	-112	14,000	10,000
25	4	-112	-123	16,000	10,000
26	5	-123	-134	18,000	10,000
27	6	-134	-145	20,000	12,000
28	7	-145	-156	22,000	16,000
29	8	-156	-167	24,000	20,000
30	9	-167	-178	26,000	25,000
31	10	-178	-189	28,000	30,000
32	11	-189	-200	30,000	35,000

* $C_i = 10*EC_{bulk}*F$, formation factor F = 4
* C_i layer 15 is based on concentrations from abstraction wells not affected by saltwater (well 242.320)

The adjusted and recalibrated model shows a slightly better model performance (Table 4-6). Model simulation with the adjusted (re-calibrated) model indicates that the advective zone extends even deeper. It is also seen that for this study area and model setup the depth of the saltwater interface changed significantly from after 50 years of simulation to after 340 years of simulations (Figure 4-9). This model phase starts in 1960 with the initiation of the major groundwater abstraction in the area in 1960.

It should be further analysed if steady state conditions has been achieved after 340 years of simulation, and how the transition and initial conditions from one model phase to the other affect the model results. Model results indicate that the salinity gradient of the transition zone is modelled quite well, but it is not located deep enough, about 15 meters too high for this specific location around borehole 242.344 (Figure 4-9). In the deeper part of the diffusion zone the modelled salinity has not changed from the initial concentrations, because the total model simulation period of 3.700 years is very short compared to the timescale of the diffusion processes (Bonnesen et al., 2009).

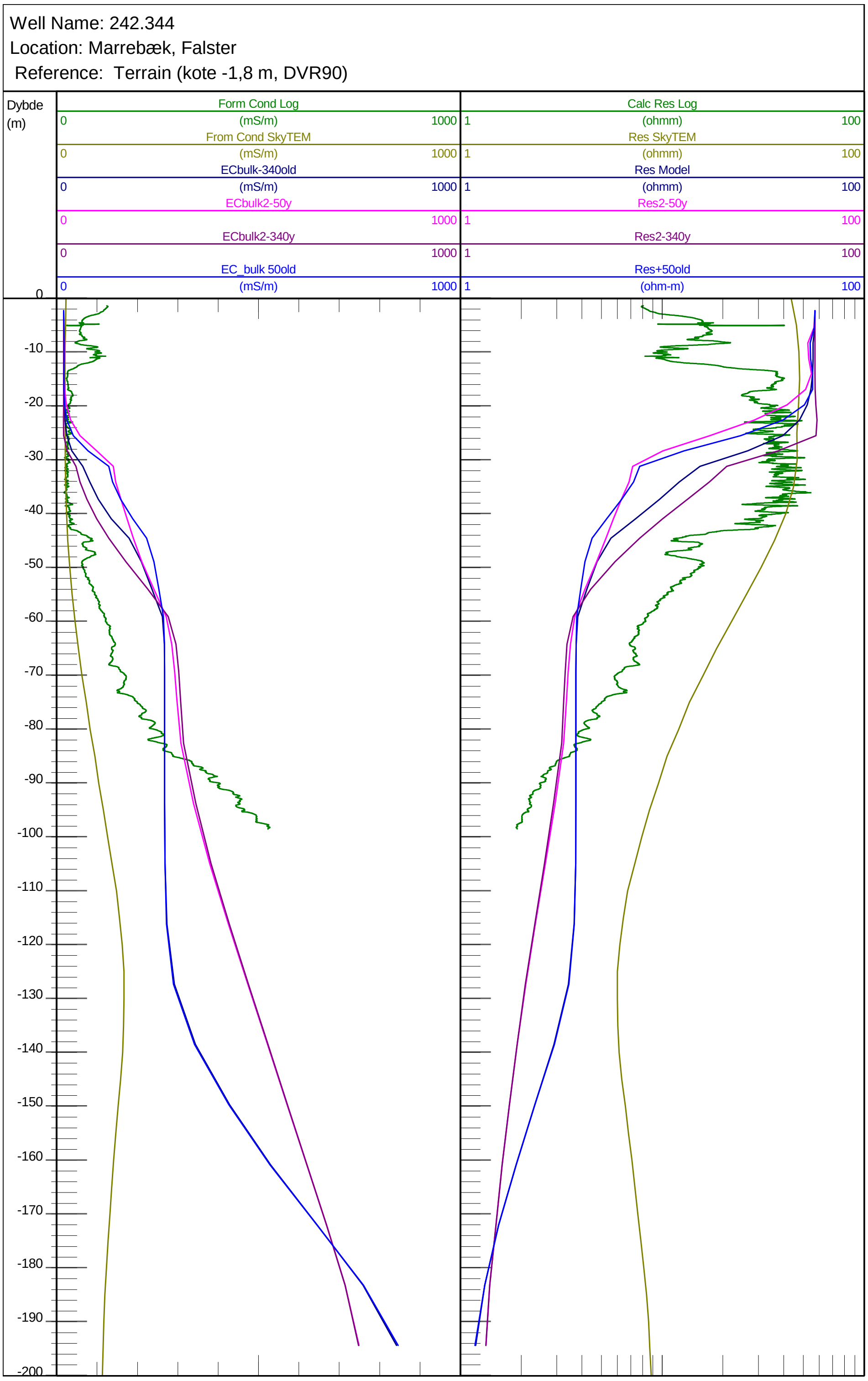

Figure 4-9. Modelled formation conductivities (left) and resistivities (right) compared to wireline logging and SkyTEM survey: 1) before recalibration: blue "… 50old", 2) after recalibration, at 50 years model simulations: red "…50y", and at 340 years model simulations: purple "…340y"

4.3.2 Using pilot points

Calibration using pilot points was tested in six different combinations of model parameters.

Test 1 and 2 were performed with hydraulic conductivities from the old model setup. Tests 3 to 6 were performed on the adjusted recalibration model (Table 4-5). 'Pre-pp07-3tr' (text marked in grey) shows the calibration statistics after implementation of the changed distribution of hydraulic conductivities to the new model. The best calibration statistics has been achieved with the smaller variogram alpha (α) (Table 4-6).

Table 4-5. Model recalibration setup (in grey 'Pre-pp07-3tr' see text above)

Calibration no.	Remarks
Manual calibration	
MarHUF008	old calibrated setup
MarHUF009	k-values layer 9 = k-values layer 8 (larger advective zone); layer 9-13: k-values moved 1 layer down
Pilot points calibration	
pp07-1tr	pilot points layer 7, 33 kx PP
pp07-2tr	change PP min, max, start value
pre-pp07-3tr	before PP run, changed Kx zone 5 and below, larger adv zone
pp07-3tr	after PP run, changed Kx zone 5 and below, larger adv zone
pp07-4tr	as -3; 67 kx PP, 39 kz PP, keep kx/kz ratio, 24 super PP
pp07-5tr	as -4; variogram α=750 (prev. run α=1500 m), 24 super PP
pp07-6tr	as -4; variogram α=2000 (prev. run α=1500 m), 24 super PP

Table 4-6. Calibration statistics for recalibration of model

Calibration no.	Residual Mean	RMS Error	dHmax	Sobs	ME/ dHmax	RMS/ Sobs	RMS/ dHmax
Manual calibration							
MarHUF008	-0.15	1.53	7.44	1.52	-0.02	1.01	0.206
MarHUF009	-0.10	1.50	7.44	1.50	-0.01	1.00	0.202
Pilot points calibration							
pp07-1tr	0.42	1.50	7.44	1.44	0.06	1.04	0.202
pp07-2tr	0.33	1.39	7.44	1.29	0.04	1.08	0.187
pre-pp07-3tr	0.50	1.64	7.44	1.56	0.07	1.05	0.220
pp07-3tr	0.44	1.45	7.44	1.38	0.06	1.05	0.195
pp07-4tr	0.50	1.64	7.44	1.56	0.07	1.05	0.220
pp07-5tr	0.39	1.30	7.44	1.23	0.05	1.06	0.175
pp07-6tr	0.50	1.43	7.44	1.33	0.07	1.08	0.192
Target crit.	-	-	-	-	0.010	1.650	0.025

The results of pilot calibration of horizontal hydraulic conductivities of model layer 7 are seen in Figure 4-10.

The calibration statistics from the pilot point calibration is similar to the results of the manual calibration based on the results of the geophysics (Table 4-6). For the injection model simulation tests the model setup from the manual recalibrated groundwater model is used.

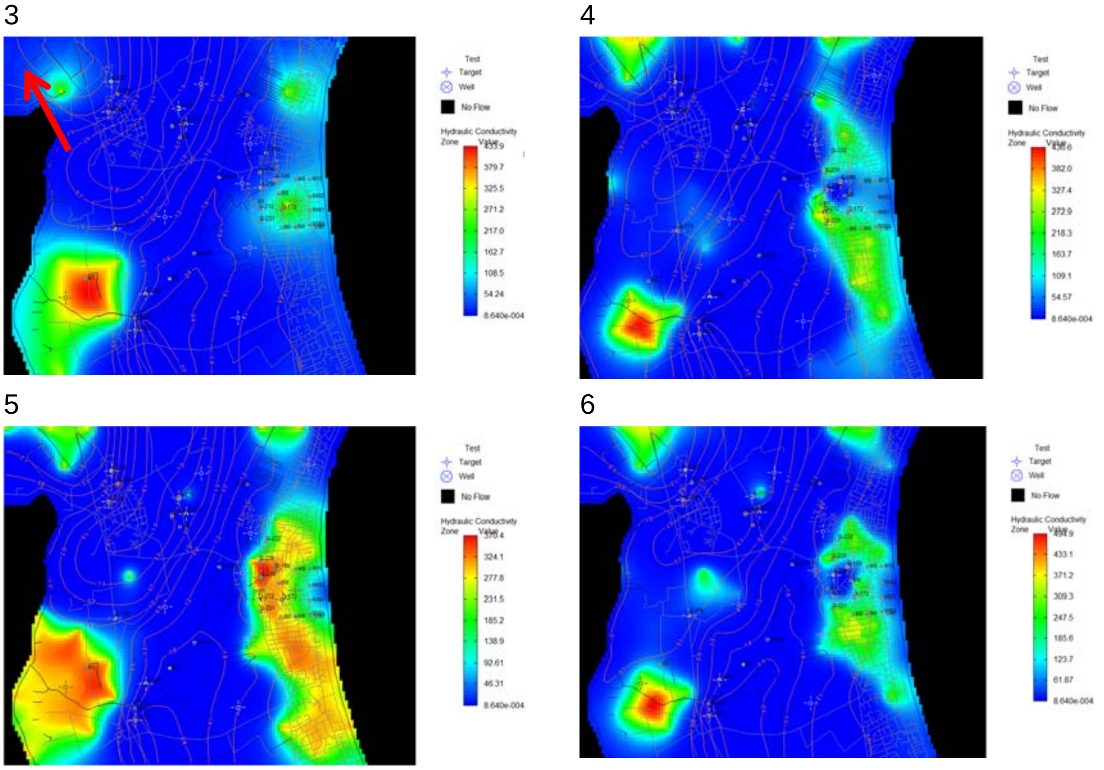

Figure 4-10. Results of pilot calibration of horizontal hydraulic conductivities of model layer 7, the number refers to the calibration setup Table 4-5. Red arrow direction is north

The results of the pilot point calibration tests indicate that a smaller correlations length results in larger heterogeneity (Figure 4-10).

4.4 Injection wells in local model

Figure 4-11 shows the results of the injection tests for two groundwater abstraction wells in the area, well no. 172 nearest the injection wells and well no. 212 further away (Figure 3-9). Table 4-6 gives an explanation for the legend in Figure 4-11. An explanation of the model setup of the injection simulations is given in section 3.3.3.

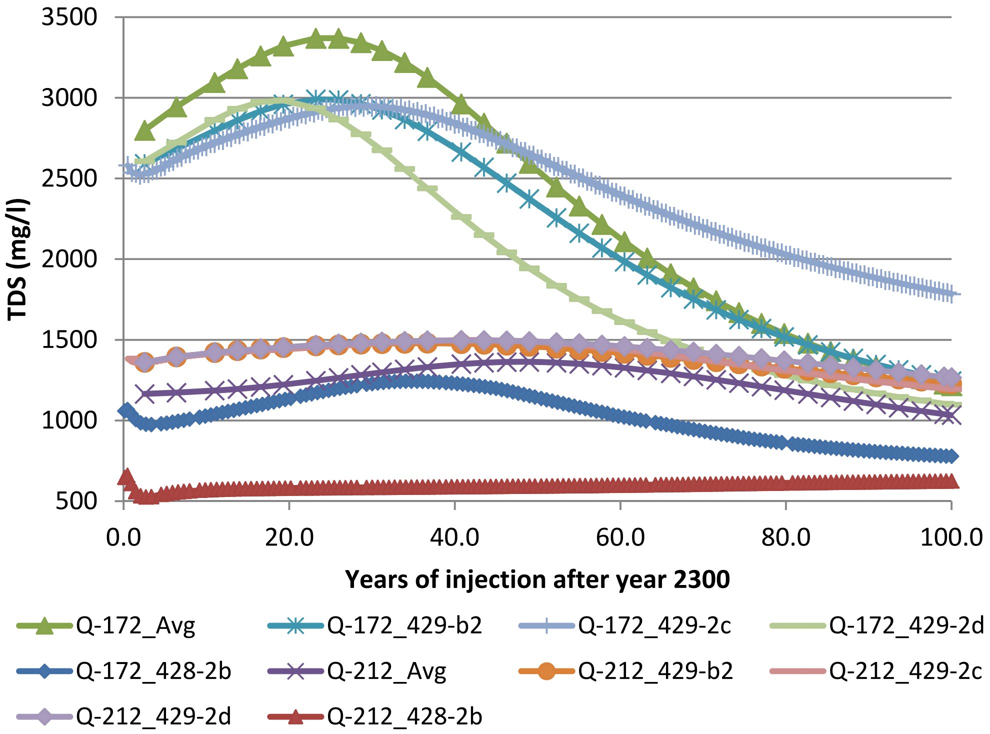

Figure 4-11. TDS concentrations in well 172 and 212 during 100 years of injection, explanation of legend see Table 4-7

Table 4-7. Explanation of the legend to Fig. 4-11 (above)

Figure 4-11 Legend	Well	Climate Scenario	Injection (m^3/d)	Remarks
Q-172_Avg	242.172	3	3 x 68	Before recalibration
Q-172_429-b2	242.172	3	3 x 68	After recalibration
Q-172_429-c2	242.172	3	½ x 3 x 68	Alternating pumping
Q-172_429-d2	242.172	3	1 x 68	Horizontal well
Q-172_428-b2	242.172	2	3 x 68	Climate scenario 2
Q-212_Avg	242.212	3	3 x 68	Before recalibration
Q-212_429-b2	242.212	3	3 x 68	After recalibration
Q-212_429-c2	242.212	3	(½ x) 3 x 68	Alternating pumping
Q-212_429-d2	242.212	3	1 x 68	Horizontal well
Q-212_428-b2	242.212	3	3 x 68	Climate scenario 2

After the model recalibration the TDS concentration in well 172 is lower than for the old model before the start of the injection period. At the end of the injection period the TDS concentration is the same for the two models. For both models the maximum concentration is seen after 25 years of injection where after the concentration decreases to around half of the initial TDS concentration. For well 212 the TDS concentration is higher in the recalibrated model than the old model before start of injection, and it continues to be so throughout the whole injection period. The maximum concentration is seen after 35 years in the recalibrated model, and 15 years later in the old model.

For the alternating injection a similar pattern is seen, but with a later maximum concentration and a higher end-concentration after 100 years of injection, the total injection is 50% of the continuous injection. With the horizontal injection well with a continuous injection of 33% of the total vertical well injection volume the increasing TDS concentration is reversed at an earlier point in time, after 20 years of injection, and the end-concentration after 100 years of injection is the lowest of the shown scenarios for well 172. Figure 4-12 shows the differences in freshwater distribution around the injection wells comparing vertical and horizontal injection wells.

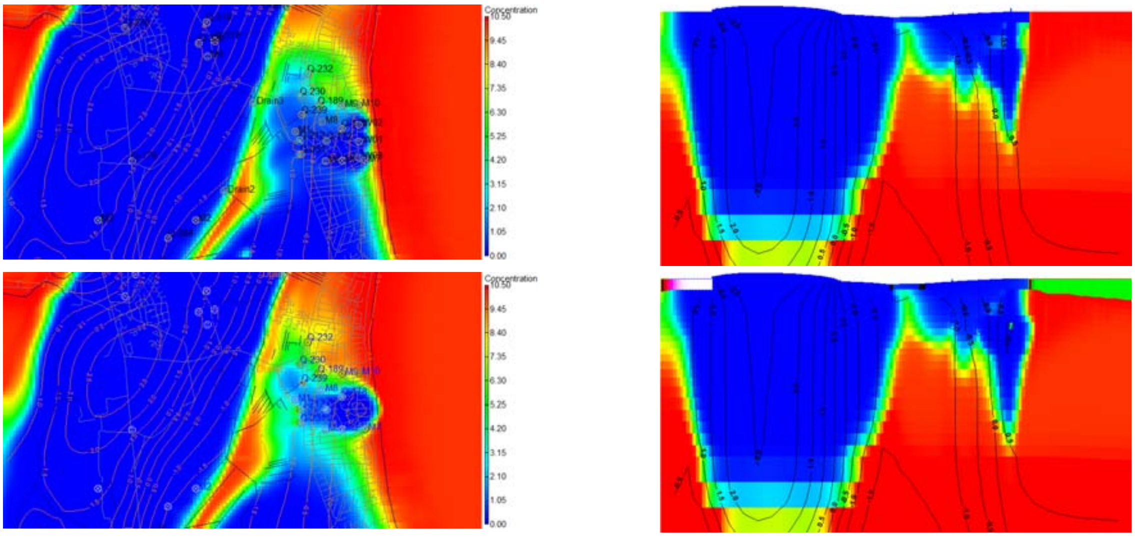

Figure 4-12. Plan view and cross section of freshwater distribution around the vertical (upper) and horizontal injection well(s) (lower)

For the less severe climate scenario 2 the TDS concentrations are lower before the start of the injection compared to scenario 3. The increasing TDS concentration in well 172 is reversed after 35 years, and ends at 50% of the start concentration after 100 years of injection. The injection has no effect on well 212, where the TDS concentration continues to increase during the whole injection period.

Notice that the TDS concentrations are the additional seawater TDS contribution to the freshwater. In the model the freshwater TDS concentration is set to be zero.

Water from the injection wells will end up in the groundwater abstraction wells. A tracer simulation indicates that after 100 years of injection half of the groundwater abstracted from the waterworks abstraction well closest to the injection well origins from the injection well. It suggests that the injection wells act more like storage, recovery and dilution of saltwater than as a hydraulic barrier against saltwater intrusion (Figure 4-13).

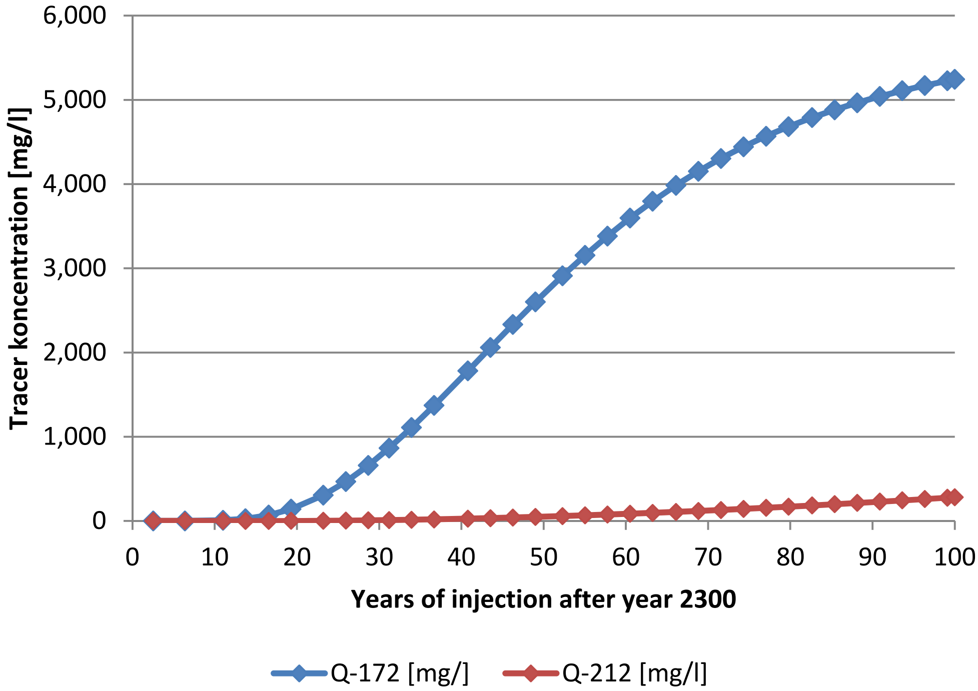

Figure 4-13. Tracer-concentration in two abstraction wells from 100 years of injection (scenario 3-b2). Concentration of injected water: 10.500 mg TDS/l

4.5 Generic models

The two generic models, the one with diffusion only and the one also with seawater intrusion, see Table 3-11, shows significant differences in saltwater transport towards the pumping well (Figure 4-14). In the generic model only including the diffusion processes all water are flowing towards the drain and the pumping well causing the saltwater concentration in the pumping well to stabilize at a lower level compared to the generic model also including seawater intrusion (Figure 4-15).

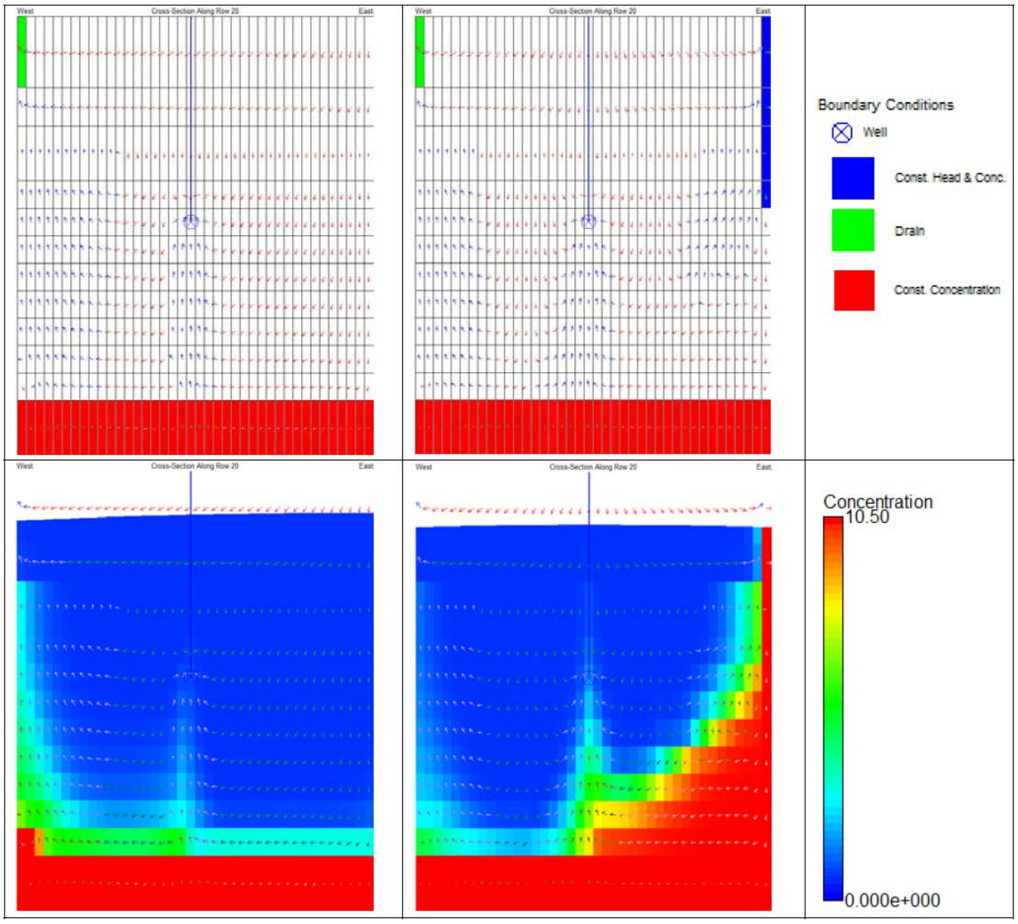

Figure 4-14. Cross sections showing flow vectors (upper) and TDS concentrations (lower) for generic model scenario 4 (left) and scenario 5 (right)

Figure 4-15 also shows that a higher diffusion coefficient, a lower hydraulic conductivity of the clay layer (the aquitard) covering the chalk aquifer, or a higher saltwater concentration in the bottom layer all results in at higher TDS concentration in the pumping well compared to the standard values (Table 3-11, scenario 1-4). In the generic models it takes more than 400 years after the start of the pumping before the TDS concentration in the well reach a constant level. The pumping well in the generic model with seawater intrusion reaches a much higher saltwater concentration after 400 years of pumping compared to the genetic models with only diffusion of saltwater from the bottom layer.

It is also seen in Figure 4-15 (scenario P1-gm05) that it takes about 250 years before saltwater originating from the seawater intrusion starts to affect the TDS concentration in the pumping well. This generic model setup does not represent a natural situation where a saltwater wedge normally has developed inland from the sea before the start of a groundwater abstraction. But the generic models illustrate the magnitude of saltwater origination from the two different sources, diffusion and seawater intrusion.

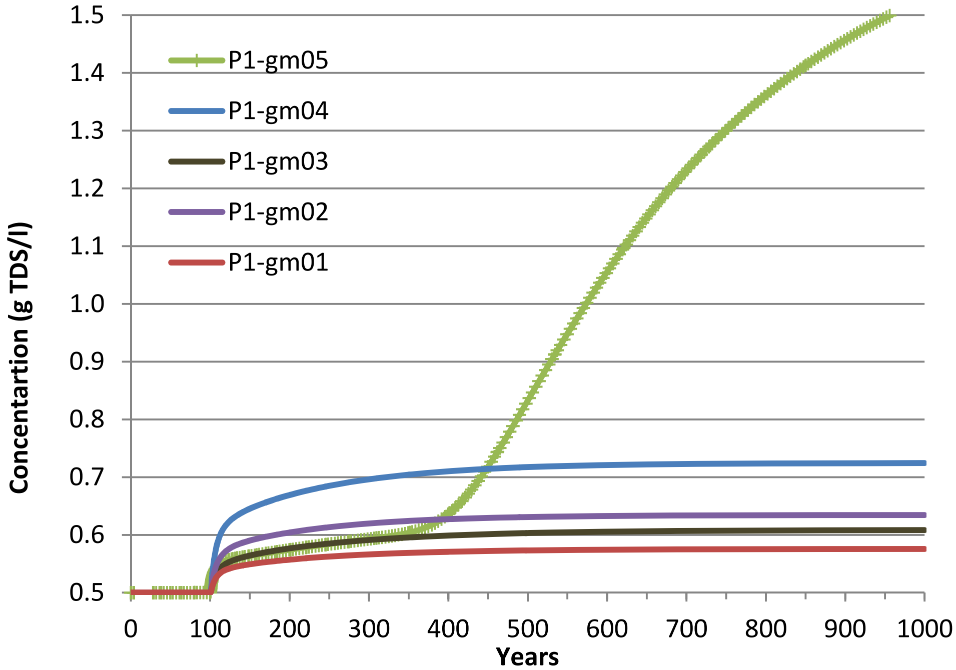

Figure 4-15. Concentration of TDS in pumping well P1 for the generic models scenario 1-5. Pumping from P1 started after 100 years (gmXY refers to the scenario number Table 3-11)

For the generic models scenarios 5-11 (Table 3-11) the results are shown as TDS concentration for the pumping well (Figure 4-16).

For scenario 6, where the seawater boundary condition is removed from the top layer of the chalk aquifer, little or no effect is seen of the seawater intrusion. In scenario 7 and 8, where a lower hydraulic conductivity is applied to the lower part of the aquifer (Figure 4-17), we also see little or no effect of seawater intrusion. The main groundwater flow towards the pumping well is taking place in the upper high conductivity layers, whereas low-conductivity layers is holding back the intruding saltwater (Figure 4-17).

Scenario 11, with a lower hydraulic conductivity of the clay aquitard, shows a higher TDS concentration in the pumping well compared to the standard scenario 5. More groundwater is drained away in the upper sand layers and less freshwater is recharging the chalk aquifer.

For the two climate change scenarios 9b and 10 (sea level rise of 0,5 m and 15% increase in groundwater recharge), the sea level rise results in an large increase in saltwater in the pumping well. An increase in recharge will for a period result in a small reduction of the TDS concentration in the pumping well, but after a longer period of pumping the concentration is the same as for the standard generic model, scenario 5 (Figure 4-16).

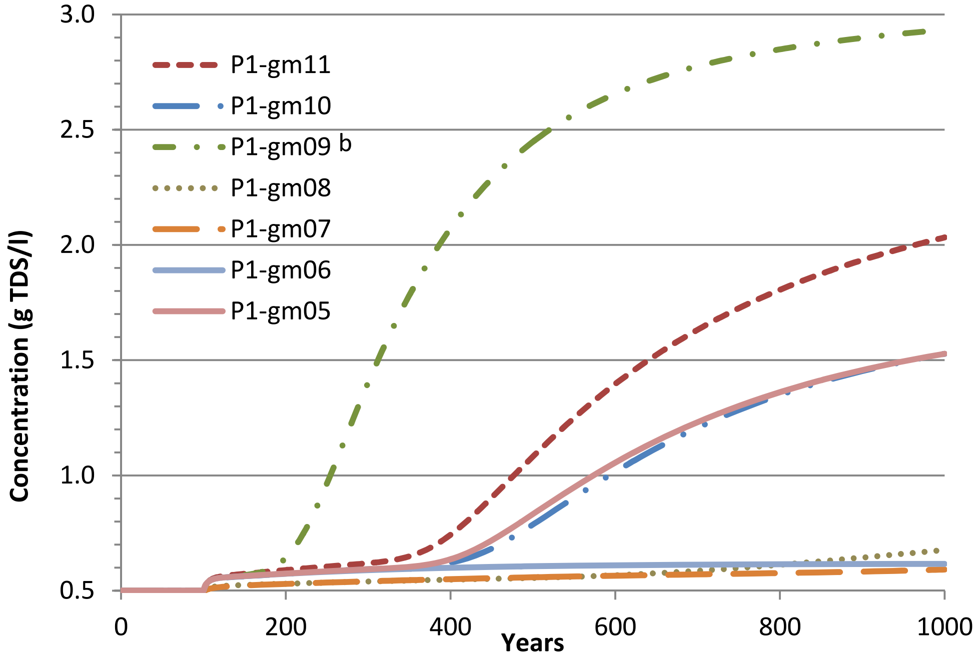

Figure 4-16. **Concentration of TDS in pumping well P1 for the generic models scenario 5-11. Pumping from P1 started after 100 years**

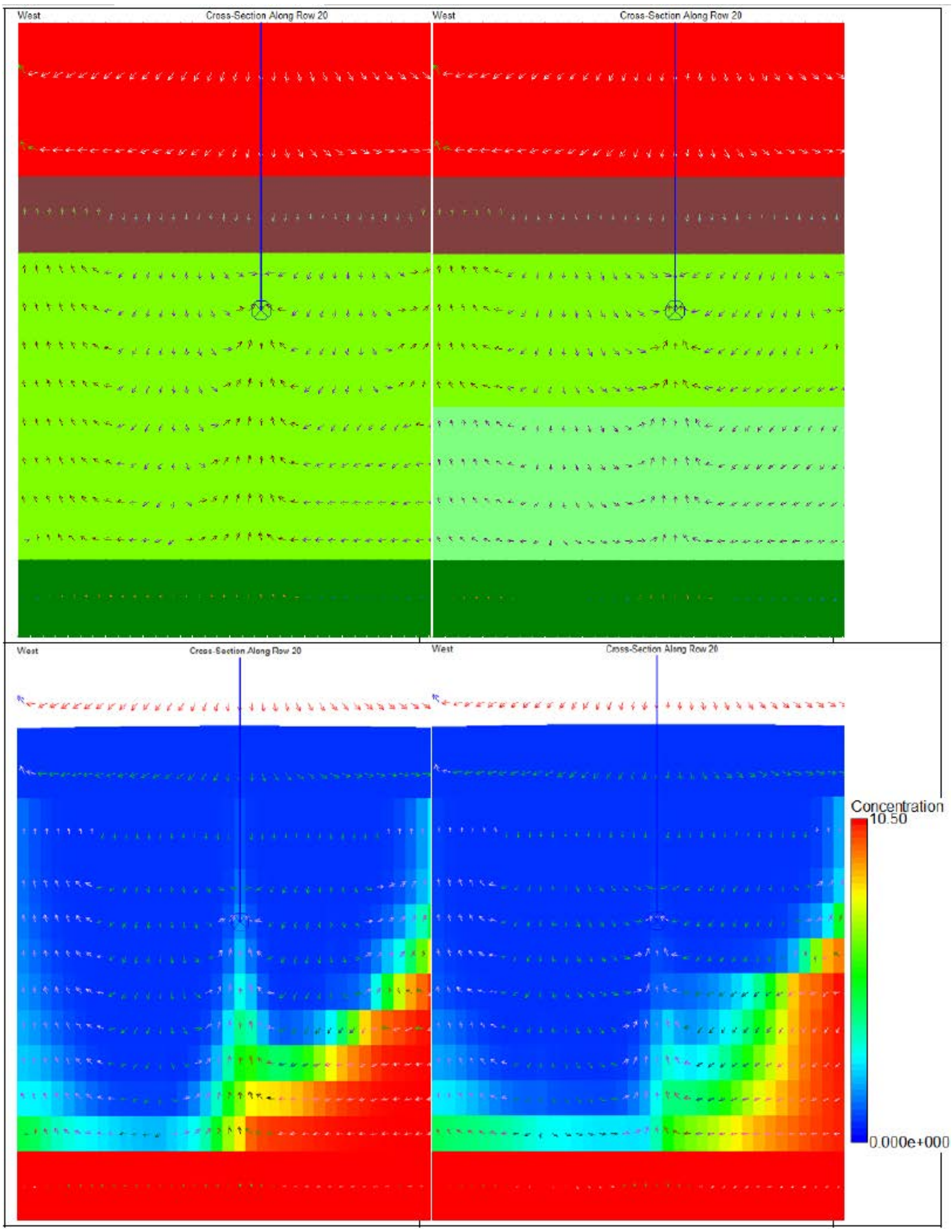

Figure 4-17. Cross sections showing flow vectors and geological layering (upper) and TDS concentrations (lower) for generic model scenario 5 (left) and scenario 8 (right)

4.5.1 Injection wells in generic models

Injection of water with no or very little concentration of salt will dilute and reduce the TDS concentration in the pumping well slightly, scenario 12 (Figure 4-18). Focusing the injection of water in one well compared to three wells (scenario 12b and 14) seems to give a slightly lower concentration for these geologically homogeneous generic models (Figure 4-18). The high injection rates used in scenario 12, 12b and 14 keeps the TDS concentration in the pumping well at low levels comparable to the concentrations found in the generic diffusion models (Figure 4-15).

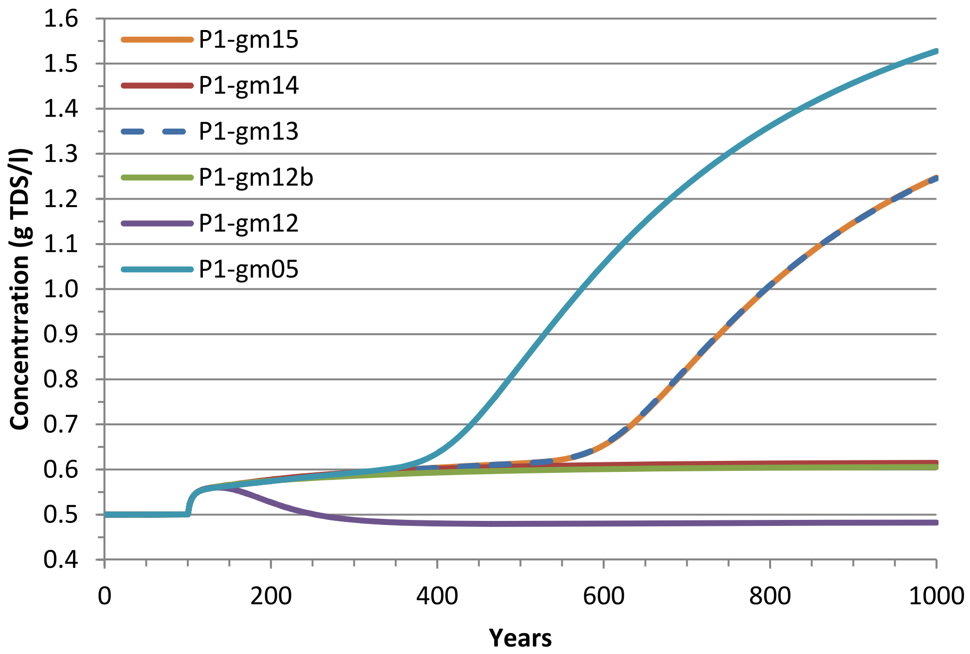

Figure 4-18. Concentration of TDS in pumping well P1 for the generic models scenario 12-15. Pumping from P1 started after 100 years

A reduced injection rate to 25% (scenario 13 and 15) is not enough to prevent the TDS concentration in the pumping well to increase after 500 years of injection. Compared to the standard generic model scenario 5 the reduced injection rate will delay the increase in TDS concentration in the pumping well by 200 years (Figure 4-18).

Using a vertical injection well (scenario 13) or a horizontal injection well (scenario 15) results for these generic models in the same TDS concentration in the pumping well (Figure 4-18). Only very minor differences in concentration distribution are seen between the vertical and the horizontal well (Figure 4-19).

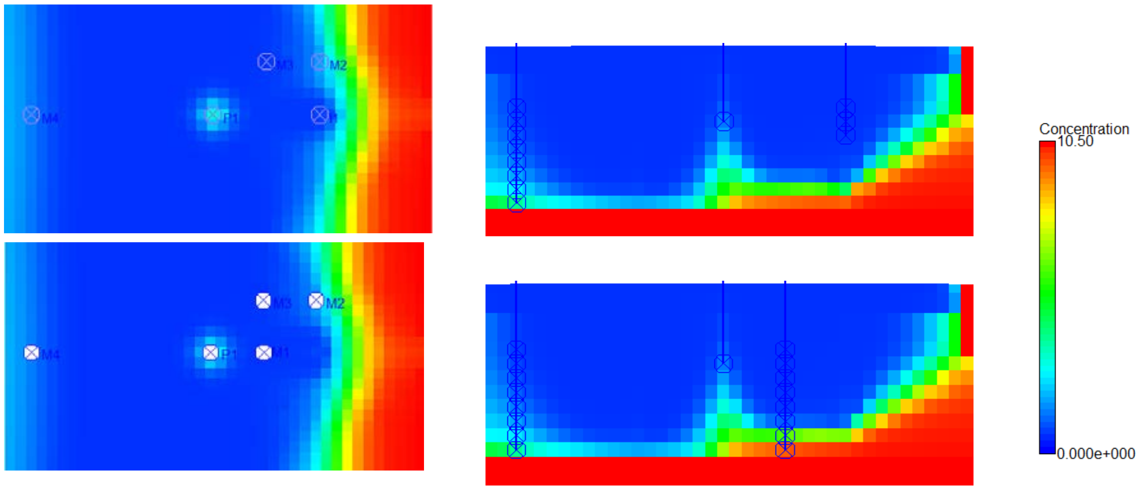

Figure 4-19. Plan view and cross section of freshwater distribution around the vertical injection well scenario 13 (upper) and horizontal injection well scenario 15 (lower)

4.5.2 Monitoring system designs

Results from the monitoring well, M1, placed between the pumping well and the sea or the injection well (Figure 3-10, 3-11) are shown in this section.

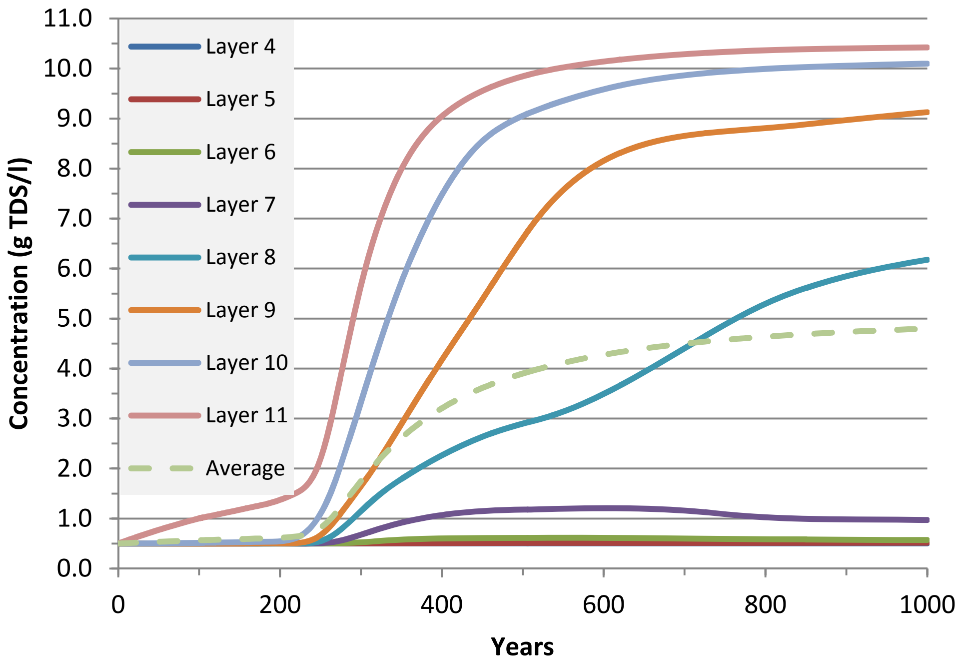

Figure 4-20. Concentration of TDS in monitoring well M1 for different model layers, generic model scenario 5. Pumping from P1 started after 100 years

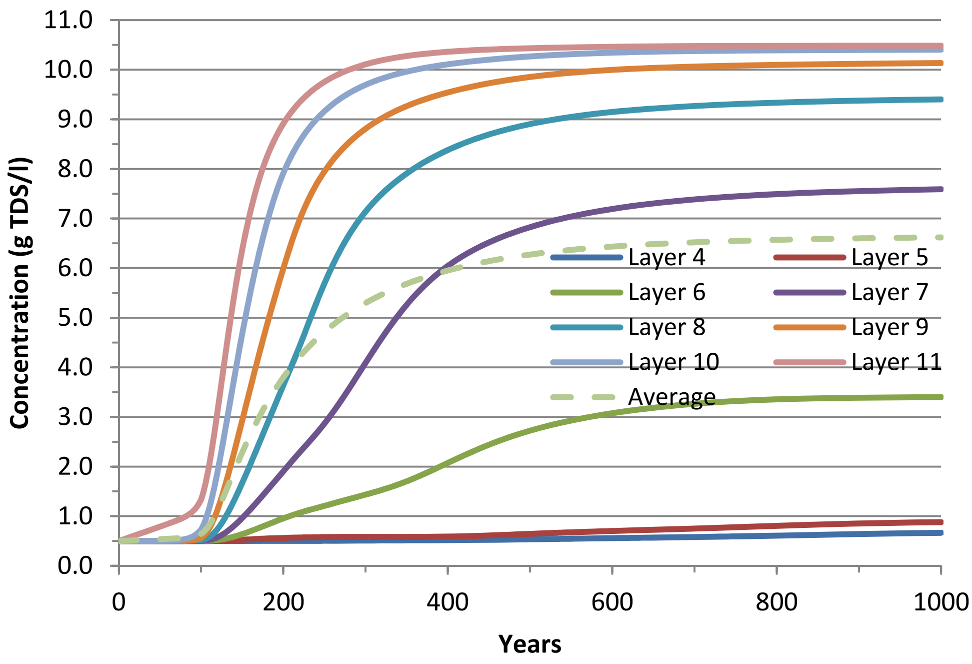

Figure 4-21. Concentration of TDS in monitoring well M1, generic model scenario 9. Pumping from P1 started after 100 years

Results from the monitoring well M1 shows that concentrations are higher in deeper layers, and that increases in TDS concentrations are seen at an earlier point in time in the deeper layers compared to the upper layers. Some upper layers are unaffected by saltwater intrusion. This picture also applies to the sea level rise scenario 9, where more layers are affected compared to scenario 5 (Figure 4-20 and 4-21). As mentioned earlier the generic model setup does not represent a natural situation where saltwater wedges normally has developed inland from the sea before the start of a groundwater abstraction, but are used to illustrated general cases.

Though the effect of a vertical injection well and a horizontal well seems to be the same for the TDS concentration in the pumping well (Figure 4-18), the saltwater concentration at different depths shows differences for the two scenarios. For the vertical injection well the seawater intrusion seems to arrive later to the monitoring well and only the three deeper layers are affected, whereas for the horizontal well more layers are affected and at an earlier time. But the horizontal well seems to prevent the saltwater from diffusion in the deepest layer 11 to reach the monitoring well (Figure 4-22 and 4-23).

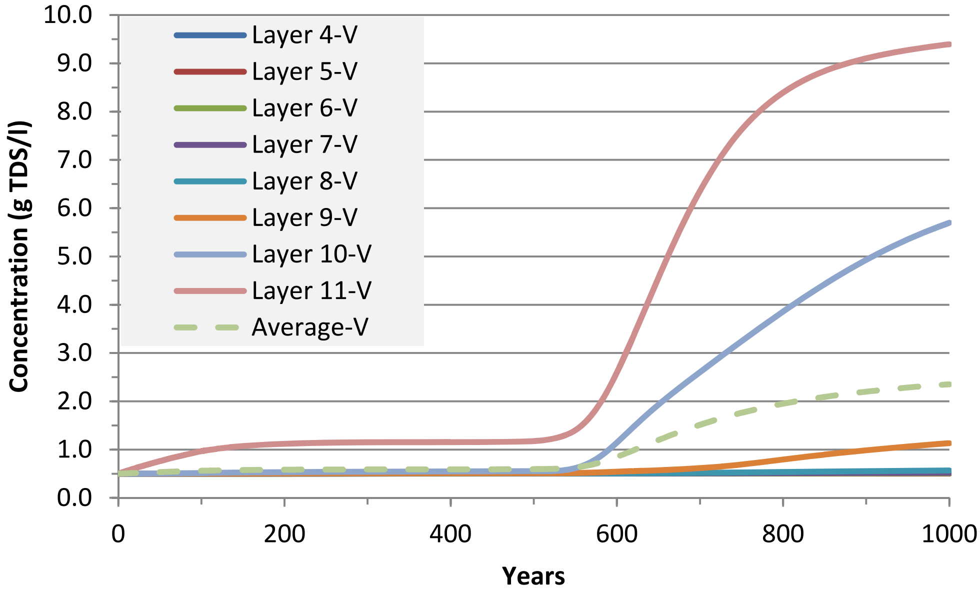

Figure 4-22. Concentration of TDS in monitoring well M1, generic model scenario 13 with 1 <u>vertical</u> injection well, I1. Injection was started at year 0

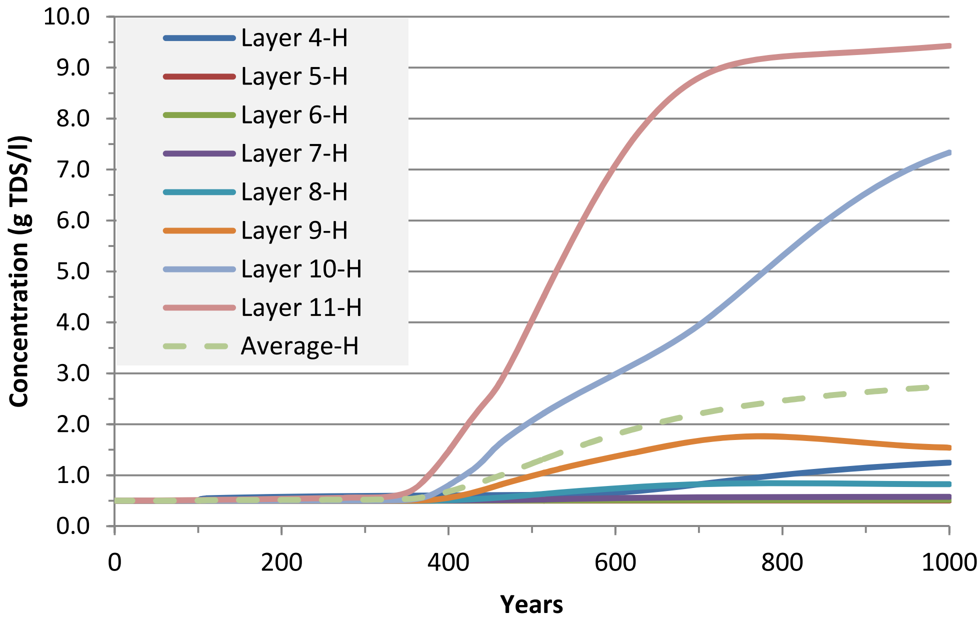

Figure 4-23. Concentration of TDS in monitoring well M1, generic model scenario 15 with 1 <u>horizontal</u> injection well. Injection was started at year 0

5. Discussion

5.1 Using geophysics for model calibration

Model results indicate that salinity gradient of the transition zone is modelled quite well, but it is not located deep enough, 15 meters too high. In the deeper diffusion zone the modelled salinity has not changed from the initial concentrations, because the total model simulation period of 3.700 years is very short compared to the timescale of the diffusion processes (Bonnesen et al., 2009).

It is also seen that for this study area and model setup the depth of the saltwater interface changed significantly from after 50 years of simulation to after 340 years of simulations, starting with the initiation of the major groundwater abstraction in the area in 1960. It should be further analysed if steady state conditions has been achieve and how the transition and initial conditions from one model phase to the other affect the model results.

5.2 Pilot point calibration

As most of the groundwater head observations in the study area are from the upper most part of the chalk aquifer, corresponding to one layer in the model, it has only been possible to perform a regular pilot point calibration for this model layer, layer 7. The calibration statistics did not show better model performance than for the manual calibration. Only a few tests were performed and the following suggestions for future work with the pilot point calibration might improve the calibration with the pilot point calibration techniques:

- The number and distribution of pilot points, both horizontally and vertically
- Analyse the effect of bounds / constraints on the pilot point parameters
- Including other hydraulic conductivity zones (model layers) in the calibration, i.e. the possible effect of changes in hydraulic conductivities for one zone (pilot point calibrated zone) might affect the hydraulic conductivity of other zones
- The used model setup was a freshwater-only sub-model of the variable density model of the whole study area.
    - o A pilot point calibration of the full variable density model for the study area is too computer time demanding that is it not realistic in the present project (Langevin and Zygnerski, 2013)
    - o A more accurate delineation of the transition zone between freshwater and saltwater to define no-flow zones in the freshwater model used for pilot point calibration.

A general pattern in the pilot point calibration tests is that the hydraulic conductivities are higher in the part of the aquifer located below the barrier island in the eastern part of area. It is also in this area that two of the water works three well fields are located. The estimated hydraulic conductivities for that area varies between 100 and 300 m/d ($1.2*10^{-3}$ – $3.5*10^{-3}$ m/s), which are relatively high values.

Around the third well field in the central/northern part of the area the hydraulic conductivities are the same as in the major part of the model area.

The interpretation of the results of the pilot point should be linked to a plausible geological structural explanation. An east – west structure is seen in the central part of the barrier island where a lowering in the surface of the chalk aquifer may coincide with a fault structure (Mathiesen et al. 2009), and a lower hydraulic conductivity according to the pilot point calibration. The high conductivity values seen in the southwest of the area is most probably related to presence of an overlaying thick clay layer and an associated dip of the top chalk layer influencing the pilot point calibration (Figure 5-1).

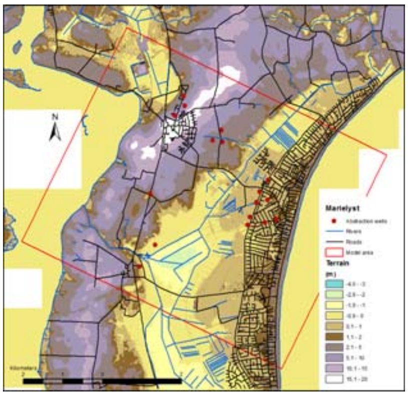

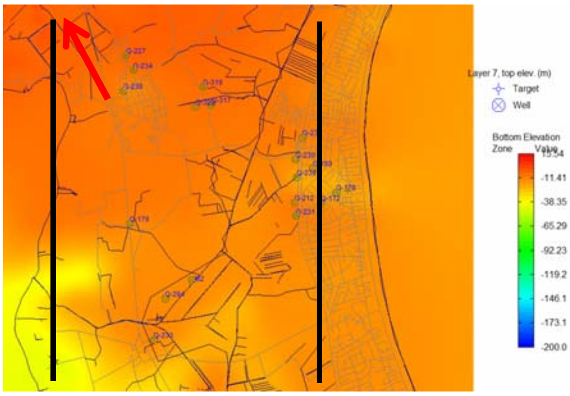

Column 15

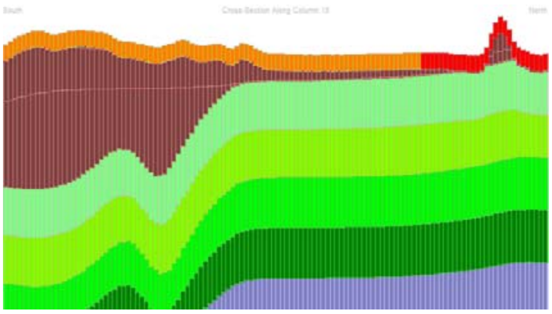

Column 104 (bottom -80 m)

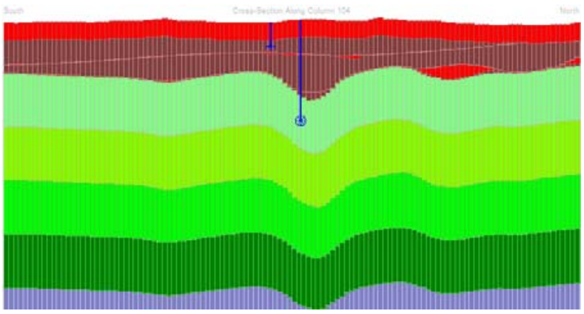

d. Faults, Denmark

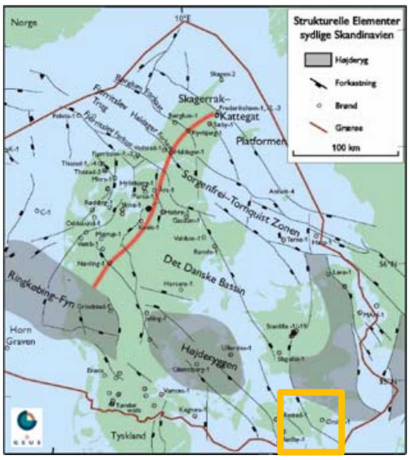

e. Faults, Falster

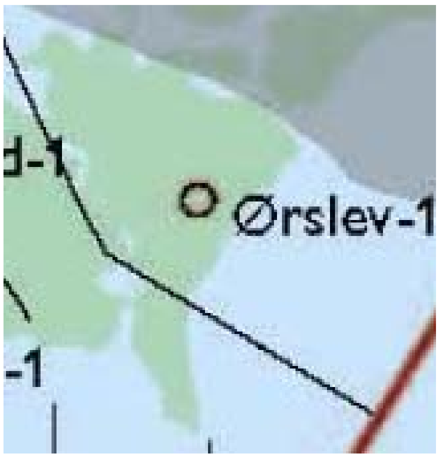

Figure 5-1. Topography, geological layering and faults in the study area

5.3 Injection wells as hydraulic barriers, local models

The present model studies have shown that a horizontal well with a length of 150 m injecting 1/3 of the water injected by three vertical wells with horizontal spacing of 300 m have a larger effect on preventing seawater intrusion. With a large vertical spacing between vertical injection wells a lot of injected water may be wasted. One other aspect that might affect the effectiveness is the vertical injection interval. For the horizontal well the injection is limited to one model layer of 3 meters thickness with high hydraulic conductivity, whereas the vertical injection wells inject water over at depth interval of 18 meters including model layers both with high and lower hydraulic conductivity.

Geological heterogeneities was only included in the injection tests to the extent of using the concept of Hydrogeologic-Unit Flow (HUF-package) transforming geological layers of varying thickness but each with a uniform hydraulic conductivity to (nearly) vertical flow model layers. The results of the pilot point test calibration suggest that it could be valuable to implement the more heterogenetic distribution of hydraulic conductivities found in the pilot point calibration in order to optimize water injection.

Alternating water injection was tested by applying an injection scheme of half year injection and half year pause. For the applied model and injection setup is seems to have very little effect on the efficiency as a hydraulic barrier. The injection rate seems to have the major effect.

Water from the injection wells will end up in the groundwater abstraction wells. A tracer simulation indicates that after 100 years of injection half of the groundwater abstracted from the waterworks abstraction well closest to the injection well origins from the injection well. It suggests that the injection wells act more like storage, recovery and dilution of saltwater than a hydraulic barrier against saltwater intrusion.

5.4 Generic models

The used generic models were based on the local model setup for the Marielyst area. The generic models have shown that saltwater from diffusion from deeper layers may increase the TDS concentrations in pumping wells by 20-40%. Depending on the aquifers contact to the sea (the boundary conditions), the effect of seawater intrusion may vary from a contribution like what was seen from diffusion to triple the TDS concentrations in pumping wells.

A lower hydraulic conductivity of the deeper part of the chalk aquifer is seen to reduce the effect of seawater intrusion in the pumping well.

Sea level rise is seen to have a much greater effect on the TDS concentration in the pumping well compared to an increase in groundwater recharge.

The test of different injection well setups with generic models indicates that the injection rate is of most importance. The relative insignificance of using 1 or 3 injections wells, or a horizontal versus a vertical well, may be because the generic model has a very homogenous geological setup.

Monitoring wells should be deep enough to be able to measure the (changes in) seawater intrusion below the freshwater lens. Monitoring wells should have monitoring points at different depth in the aquifer. Even in the geological homogenous generic models show major differences is in TDS concentrations at different depths.

6. Acknowledgement

This project was part-funded by the Danish Eco-Innovation program of the Danish Ministry of the Environment. Additional funds were obtained from the Geological Survey of Denmark and Greenland, a sector research institute within the Danish Ministry of Energy, Utilities and Climate.

7. References

Appelo, C.A.J. and Postma, D. 2005. Geochemistry, groundwater and pollution, 2nd edn. Balkema, Leiden, The Netherlands.

Bonnesen, E. P., Larsen, F., Sonnenborg, T. O., Klitten, K., and Stemmerik, L. 2009. Deep saltwater in Chalk of North-West Europe: origin, interface characteristics and development over geological time, Hydrogeol. J., 17, 1643–1663.

Carrera, J., Hidalgo, J. J., Slooten, L. J., and Vazquez-Sune, E. 2010. Computational and conceptual issues in the calibration of seawater intrusion models, Hydrogeology Journal 18: 131–145.

Christensen, S. and Doherty, J. 2008. Predictive error dependencies when using pilot points and singular value decomposition in groundwater model calibration. Advances in Water Resources 31: 674–700.

Comte, J. and Banton, O. 2007. Cross-validation of geo-electrical and hydrogeological models to evaluate seawater intrusion in coastal aquifers, Geophys. Res. Lett., 34, L10402, doi:10.1029/2007GL029981.

Dausman, A.M., Doherty, J., Langevin, C.D. and Dixon, J. 2010. Hypothesis testing of buoyant plume migration using a highly parameterized variable-density groundwater model at a site in Florida, USA. Hydrogeology Journal 18: 147–160 DOI 10.1007/s10040-009-0511-6.

David, R. and Pyne, G. 2005. Aquifer Storage Recovery. A guide to groundwater recharge through wells. Second Edition. ASR Systems LLC, Gainesville, Florida, U.S.A.

GeofysikSamarbejdet, 2011. Himmerland - Vurdering af SkyTEM metoden til sårbarhedskortlægning. Aarhus Universitet, juli 2011.

He, X., J. Koch, T. O. Sonnenborg, F. Jørgensen, C. Schamper, and J. Christian Refsgaard. 2014. Transition probability-based stochastic geological modeling using airborne geophysical data and borehole data, Water Resour. Res., 50, 3147–3169, doi:10.1002/2013WR014593.

Kaleris, V.K. and Ziogas, A.I. 2013. The effect of cutoff walls on saltwater intrusion and groundwater extraction in coastal aquifers. Journal of Hydrology 476: 370–383. http://dx.doi.org/10.1016/j.jhydrol.2012.11.007.

Klitten K. and Wittrup CS. 2006. Undersøgelser af saltvandsgrænsen ved hjælp af geofysisk borehulsloging. Saltvandsgrænsen i kalkmagasinerne i Nordøstsjælland, delrapport 2. GEUS Rapport 2006/17 (in Danish).

Langevin, C.D. and Zygnerski, M. 2013. Effect of Sea-Level Rise on Salt Water Intrusion near a Coastal Well Field in Southeastern Florida. Groundwater, Vol. 51, No. 5, September-October 2013 (pages 781–803).

Larsen F, Sonnenborg T, Madsen P, Ulbak AU and Klitten K. 2006. Saltvandsudvaskning i Danienkalk og Skrivekridt: detailundersogelser i Karlslunde vaerkstedsomraade [Saltwater transport in the Danian Limestone and Chalk: detailed studies from Karlslunde study area]. Partial report no. 6, 2006/21, The Geological Survey of Denmark and Greenland, Copenhagen, pp 1–103.

Maneta, M.P. and Wallender, W.W. 2013. Pilot-point based multi-objective calibration in a surface–subsurface distributed hydrological model. Hydrological Sciences Journal, 58:2, 390-407, DOI: 10.1080/02626667.2012.754987

Mathiesen, A., Kristensen L., Bidstrup, T., Nielsen, L.H. 2009. Vurdering af det geotermiske potentiale i Danmark. GEUS Rapport 2009 / 59 (in danish).

Misut. P.E. and Voss, C.I. 2007. Freshwater–saltwater transition zone movement during aquifer storage and recovery cycles in Brooklyn and Queens, New York City, USA. Journal of Hydrology 337, 87– 103. doi:10.1016/j.jhydrol.2007.01.035.

Naturstyrelsen Roskilde, 2011. SkyTEM kortlægning af Nord- og Midtfalster. Rapport. COWI. Februar 2011 (in Dansh).

Pool, M. and Carrera, J. 2010. Dynamics of negative hydraulic barriers to prevent seawater intrusion. Hydrogeology Journal 18: 95–105. DOI 10.1007/s10040-009-0516-1.

Rasmussen, P., Sonnenborg, T.O. and Hinsby, K.: Evaluating hydraulic barriers for reducing and controlling saltwater intrusion in a changing climate. Poster. SWIM 23rd Salt-Water Intrusion Meeting, June 16-20 2014, Husumhus, Husum, Germany, 2014.

Rasmussen, P., Sonnenborg, T.O., Goncear, G. and Hinsby, K.: Assessing impacts of climate change, sea level rise, and drainage canals on saltwater intrusion to coastal aquifer. HYDROLOGY AND EARTH SYSTEM SCIENCES Volume: 17 Issue: 1 Pages: 421-443, 2013.

Refsgaard, JC; Christensen, S; Sonnenborg, TO; Seifert D; Højberg, AL; Troldborg, L.: Review of strategies for handling geological uncertainty in groundwater flow and transport modeling. ADVANCES IN WATER RESOURCES Volume: 36 Special Issue: SI Pages: 36-50, 2012.

Rumbaugh, J. 2013. Webinar: Calibrating Models with PEST and Groundwater Vistas. 4-14 November 2013. Environmental Simulations, Inc.

Steiness, M. 2011. Undersøgelse af hydrologiske forhold for et kystnært vandindvindingsområde. Sydfalster. Institut for Geografi og Geologi Københavns Universitet (unpublished student project, in Danish).

Storstrøms Amt, 2000. Indsatsområde Sydfalster, Delområde 2. Geologisk detailkortlægning og konceptuel geologisk model. COWI. Maj 2000 (in Danish).

Sulzbacher, H., Wiederhold, H., Siemon, B., Grinat, M., Igel, J., Burschil, T., G¨unther, T., and Hinsby, K.: Numerical modelling of climate change impacts on freshwater lenses on the North Sea Island of Borkum using hydrological and geophysical methods, Hydrol. Earth Syst. Sci., 16, 3621–3643, doi:10.5194/hess-16-3621-2012, 2012.

Thorn, P. 2011. Groundwater salinity in Greve, Denmark: determining the source from historical data. Hydrogeology Journal 19: 445–461. DOI 10.1007/s10040-010-0680-3.

Thorn, P. and Mortensen, J, 2012. Simple Chloride Sensors for Continuous Groundwater Monitoring. Ground Water Monitoring & Remediation 32, no. 2, Spring 2012, pages 40–47. doi: 10.1111/j1745–6592.2011.01384.x.

Ward, J.D., Simmons, C.T., Dillon, P.J., 2008. Variable-density modelling of multiple-cycle aquifer storage and recovery (ASR): importance of anisotropy and layered heterogeneity in brackish aquifers. Journal of Hydrology 356, 93–105. doi:10.1016/j.jhydrol.2008.04.012

Ward, J.D., Simmons, C.T., Dillon, P.J., and Pavelic, P. 2009. Integrated assessment of lateral flow, density effects and dispersion in aquifer storage and recovery. Journal of Hydrology, 370:83–99. doi:10.1016/j.jhydrol.2009.02.055.

Zuurbier, K.G., W.J. Zaadnoordijk & P.J. Stuyfzand, 2014. How multiple partially penetrating wells improve the freshwater recovery of coastal aquifer storage and recovery (ASR) systems: A field and modeling study. Journal of Hydrology, 509: 430-441.

Appendices

Appendix 1: SWIM23 Extended abstract

Appendix 2: SWIM23 Poster

Appendix 3: Well record for borehole DGU nr. 242.375

Appendix 1: SWIM23 Extended abstract

Evaluating hydraulic barriers for reducing and controlling saltwater intrusion in a changing climate

Per Rasmussen[1], Torben O. Sonnenborg[1] and Klaus Hinsby[1]
[1]Dept. of Hydrology, Geol. Survey of Denmark and Greenland, Copenhagen, Denmark.

ABSTRACT

Groundwater abstraction from coastal aquifers is vulnerable to sea level rise, increasing groundwater abstraction and drainage because they may potentially impact saltwater intrusion and hence groundwater quality depending on the hydrogeological setting. In the present study the impacts of sea level rise, drainage systems and changes in groundwater abstraction are quantified for an island located in the Western Baltic Sea using the modeling packages MODFLOW/MT3DMS/SEAWAT. Increasing chloride concentrations have been observed in several abstraction wells indicating that saltwater intrusion is ongoing. The water resources on the island are abstracted from a confined chalk aquifer. In order to prevent saltwater intrusion a hydraulic barrier is established. The effectiveness of the barrier consisting of injection wells is examined for a projected climate change scenario using variable density modeling.

INTRODUCTION

Groundwater abstracted from coastal aquifers is at risk of increased saltwater intrusion as an effect of the projected climate changes. This problem is studied for an area located in the southeastern part of Denmark on the island of Falster in the Baltic Sea (Figure 1). The local waterworks abstract groundwater from a shallow chalk aquifer. Part of the aquifer is located near the coast where an increasing chloride concentration has been monitored in groundwater abstraction wells over the last decades (Rasmussen et al. 2013).

In some coastal areas where saltwater intrusion has been threatening groundwater well fields, injection wells have been installed to generate a hydraulic barrier that prevents further saltwater intrusion, e.g. in Spain and USA. Climate changes might cause, among other things, sea level rise and changes in groundwater recharge. The objective of the present study is to conduct a model analysis of the effect of injecting freshwater into the groundwater aquifer to act as a hydraulic barrier to prevent further saltwater intrusion in a climate change scenario with increasing sea level and reduced groundwater recharge.

METHODS

The groundwater abstraction wells in focus are located on a barrier island between the Baltic Sea to the east and a low laying drained area to the west (Figure 1). A previous model study has examined possibly effects of increasing sea level, changes groundwater recharge, and canal stage on groundwater quality (Rasmussen et al. 2013). The model area of 44km^2 is discretized using a grid size of 50m by 50m, and 32 model layers varying in thickness from 2m to 12m down to a depth of -200m.a.s.l. The main aquifer consists of fractured and crushed calk overlain by up to 45m of clayey till and sand.

In order to model the historical changes the study area has undergone from an area with saltwater lagoon and barrier islands to reclaimed and drained land with groundwater abstraction, a modeling period of more than 3000 years were carried out in order to reach a steady-state situation for the freshwater-saltwater distribution. From 1960 groundwater abstraction was implemented in the model. The modeling packages MODFLOW/MT3DMS/ SEAWAT were used for the variable density modeling.

Eight combinations of sea level rise (0.5m, 0,75m, and 1m), changed groundwater recharge (decrease of 15%, increase of 15%), and changed canal stage (-30cm, +30cm) were analyzed. The climate change effects of sea level rise and changed recharge was gradually implemented in the model form 2010 to 2100. The model simulations were continued for additionally 200 years to year 2300.

It was found that the most severe scenario concerning the chloride concentration in groundwater abstraction wells were the scenario with a 0.75m sea level rise and a decrease in groundwater recharge of 15%. This "worst case" scenario has been used for the present study.

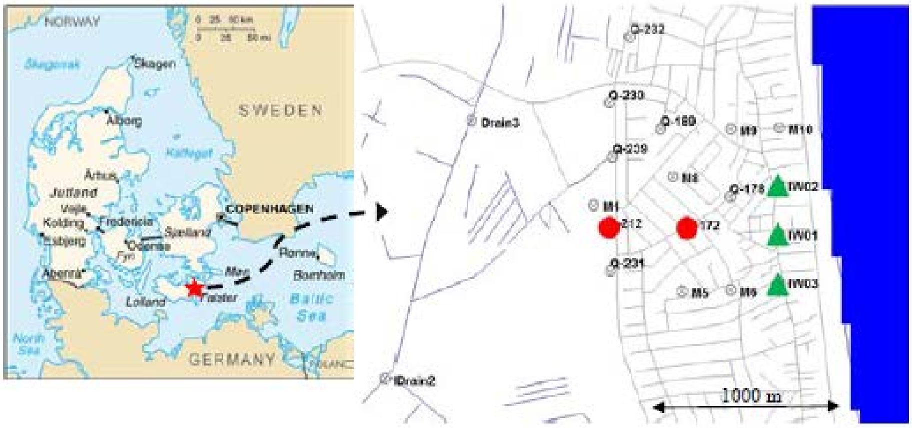

Figure 1. Location of study area (red star on left panel). Right panel shows part of the study area with two abstraction wells (red dots) and three injection wells (green triangles).

Three injection wells were added in the area between the well field and the cost line (Figure 1). The injection wells were located so far from the coast that they were not penetrating the saltwater wedge. The wells were screened in the upper fractured chalk from an elevation of -12m to -30m. The injection rates were the same as the average abstraction rates for the waterworks wells, 68 m^3/d. The injection wells are located 300m from the coast with spacing of 250m. The abstraction wells of interest for this study, Q-172 and Q-212, are located 750m and 1150m, respectively, from the coastline (Figure 1).

The injection of water in the three injections wells was started in year 2300 and the simulation was continued for additional 100 years. The salinity concentrations were monitored in the two abstraction wells, Q-172 and Q-212 (Figure 1).

RESULTS

100 years of freshwater injection has a significant effect on the extension of the freshwater lens in both horizontal and vertical direction. Figure 2 upper panels show the freshwater-saltwater distribution in the year 2300 before start of the injection. Figure 2 lower panels show the freshwater-saltwater distribution after 100 years of freshwater injection.

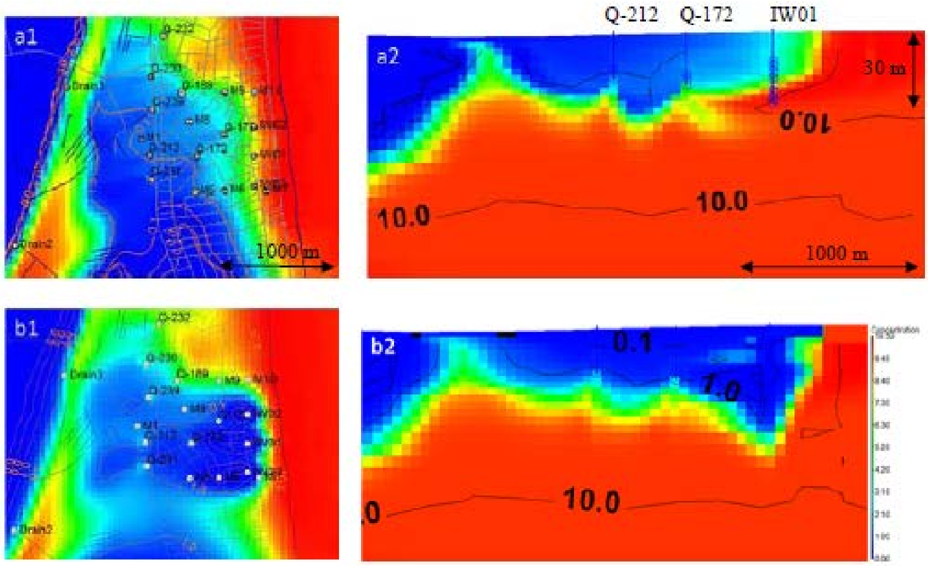

Figure 2. Saltwater distribution, plan view and cross section. Plan view: model layer 8, elevation -22m. Cross sections through wells Q-212, Q-172, and IW01. Panel a1 and a2: before injection. Panel b1 and b2: after 100 years injection. Contours: TDS (g/l).

The spacing between the three injection wells is seen to be sufficiently close to preventing saltwater intrusion between the injection wells.

Figure 3 shows the effect of the freshwater injection on TDS concentration in the two abstraction wells, Q-172 and Q-212. In the left panel the effects of the climate scenario implemented from year 2011 to 2300 is shown. The right panel shows the effect on TDS concentrations during 100 years of water injection starting in the year 2300. The effect of the injection well is first observed in the abstraction well closest to the injection wells and the coast, Q-172, after 25 years. In the abstraction well located further from the injection wells and the coast, Q-212, the effect is seen after 50 years. In well Q-172 a significant reduction in TDS concentration is found through the rest of the injection period. After 100 years of injection, the TDS concentrations are reduced to a level that is close to the concentrations found before the effects of the climate changes commenced.

However, the negative effects of climate changes could have been avoided if the injection wells had been installed before the onset of sea level rise and reduction in groundwater recharge.

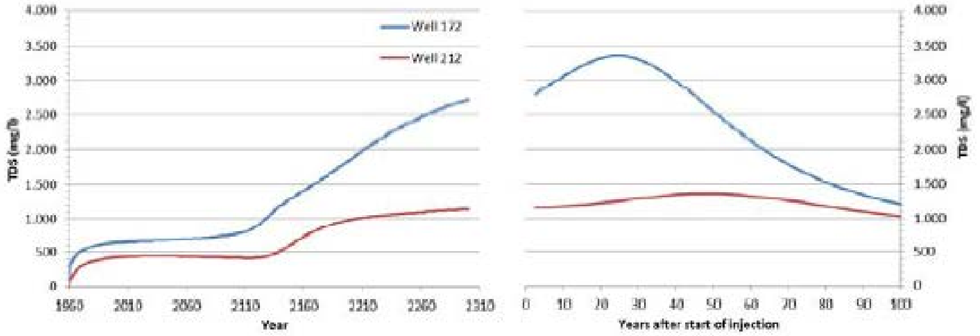

Figure 3. Effect of injection wells on TDS concentration in two groundwater abstraction wells. Location of wells, see figure 1. Left panel shows effects of a climate scenario implemented from year 2011. Right panel shows effect on TDS concentrations of 100 years water injection starting in the year 2300.

DISCUSSION AND CONCLUSIONS

Injection wells are tested as a hydraulic barrier to alleviate increased saltwater intrusion into coastal aquifers due to effects of projected climate change effects. Variable density modeling studies shows that fresh water injected into a coastal aquifer can prevent further increase in chloride concentrations in abstracted groundwater. The effectiveness of the hydraulic barrier in reversing the increasing trend in chloride concentrations in groundwater abstraction wells depends among other things on the timing of the injection scheme installation relative to the timing of climate changes.

Further studies in the area are planned to characterize the variation in hydraulic conductivity by calibrating the variable density model against available data on hydraulic head and chloride concentration using the pilot points method. Results from an airborne electromagnetic survey (SkyTEM) will be used to estimate the chloride concentration in the aquifers and it will be tested if these data can be used as targets in the calibration process. Also different designs of the hydraulic barrier including the number of injection wells, the injection rate and the location and orientation of the wells will be examined.

REFERENCES

P. Rasmussen, T. O. Sonnenborg, and K. Hinsby. 2013. Assessing impacts of climate change, sea level rise, and drainage canals on saltwater intrusion to coastal aquifer. Hydrol. Earth Syst. Sci., 17, 421–443, 2013. www.hydrol-earth-syst-sci.net/17/421/2013/. doi:10.5194/hess-17-421-2013.

Contact Information: Per Rasmussen. Geological Survey of Denmark and Greenland (GEUS), Department of Hydrology. Øster Voldgade 10, DK-1350 Copenhagen K. Phone: +45 91 33 36 33, E-mail: pr@geus.dk

Appendix 2: SWIM23 Poster

WATER4COASTS

23rd Saltwater Intrusion Meeting, 2014
Husum, Germany

GEUS

Evaluating hydraulic barriers for reducing and controlling saltwater intrusion in a changing climate

Per Rasmussen[1], Torben O. Sonnenborg[1] and Klaus Hinsby[1]
[1]Dept. of Hydrology, Geological Survey of Denmark and Greenland
Copenhagen, Denmark

1. Introduction

Groundwater abstracted from coastal aquifers is at risk of increased saltwater intrusion as an effect of projected climate changes.

A variably density model analysis is used to analyze the effect of injecting freshwater: using groundwater wells a hydraulic barriers.

Looking at climate change scenarios with increasing sea level and changing groundwater recharge.

2. Methodology

The modeling packages MODFLOW/ MT3DMS/ SEAWAT are used for the variable density modeling of transition phases in study area (Fig. 1).

Phase five includes projected climate change scenarios of sea level rise and changed groundwater recharge.

A phase seven includes a later hundred years period of freshwater injections.

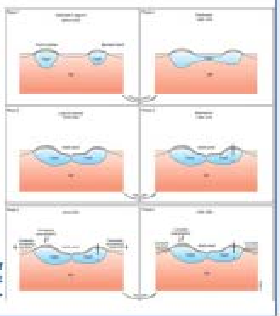

Fig 1. Modeled changes of study area (Rasmussen et al., 2013).

3. Field site

The study area is located in the south-eastern part of Denmark on the island of Falster in the Baltic Sea (Fig. 2).

The local waterworks abstract groundwater from a shallow coastal chalk aquifer.

Three synthetic injection wells are added to the groundwater model in the area between the well field and the cost line.

Fig 2. Location of study area (left panel) and location of abstraction wells (red dots, right panel) and synthetic injections wells (green triangles, right panel).

4. Model setup

The three synthetic injection wells: 300m from coast, 250m spacing, injection rates as waterworks abstraction rates (68 m³/d), well screens in the upper fractured chalk -12 to -30 masl.

The injection of water in the three modeled injections wells is started in year 2300 and the simulation is continued for additional 100 years.

5. Results

100 years of fresh-water injection has significant effect on the extension of the freshwater lens in both horizontal and vertical direction (Fig. 3).

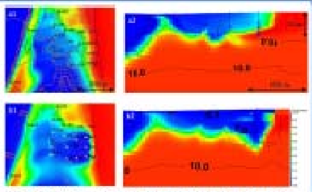

Fig 3. Saltwater distribution, plan view and cross section. Plan view: model layer 8, elevation -22m. Panel a1 and a2: before injection. Panel b1 and b2: after 100 years injection. Contours: TDS (g/l).

Negative effects of climate changes can be avoided if injection wells are installed before the onset of sea level rise and reduction in ground-water recharge (Fig. 4).

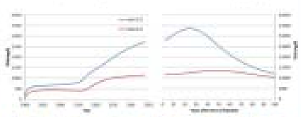

Fig 4. Effect of injection wells on TDS concentration in two groundwater abstraction wells. Left panel: effects of a climate scenario implemented 2011 to 2100. Right panel: effect on TDS concentrations of 100 years water injection starting in the year 2300.

The climate change scenario used:

- 0.75m sea level rise
- -15% groundwater recharge

6. Conclusions and future plans

Variable density modeling studies shows that fresh water injected into a coastal aquifer can prevent further increase in chloride concentrations in abstracted groundwater in a changing climate.

The effectiveness of the hydraulic barrier depends on e.g. the timing of the injection relative to the timing of climate changes.

Future studies:

- Characterize the hydraulic conductivity by calibrating model against hydraulic head and chloride concentration using the pilot points method
- Use results from geophysical surveys (MEP, SkyTEM, logging) to estimate the chloride concentrations for targets in the PP calibration
- Effect of different designs of hydraulic barriers.

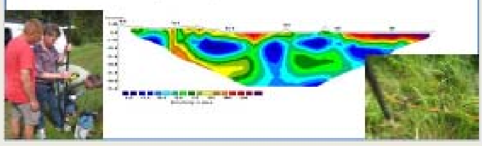

7. References

P. Rasmussen, T. O. Sonnenborg, and K. Hinsby. 2013. Assessing impacts of climate change, sea level rise, and drainage canals on saltwater intrusion to coastal aquifer. Hydrol. Earth Syst. Sci., 17, 421–443, 2013. www.hydrol-earth-syst-sci.net/17/421/2013/. doi:10.5194/hess-17-421-2013.

GEOLOGICAL SURVEY OF DENMARK AND GREENLAND   WWW.GEUS.DK

Appendix 3: Well record for borehole DGU nr. 242.375

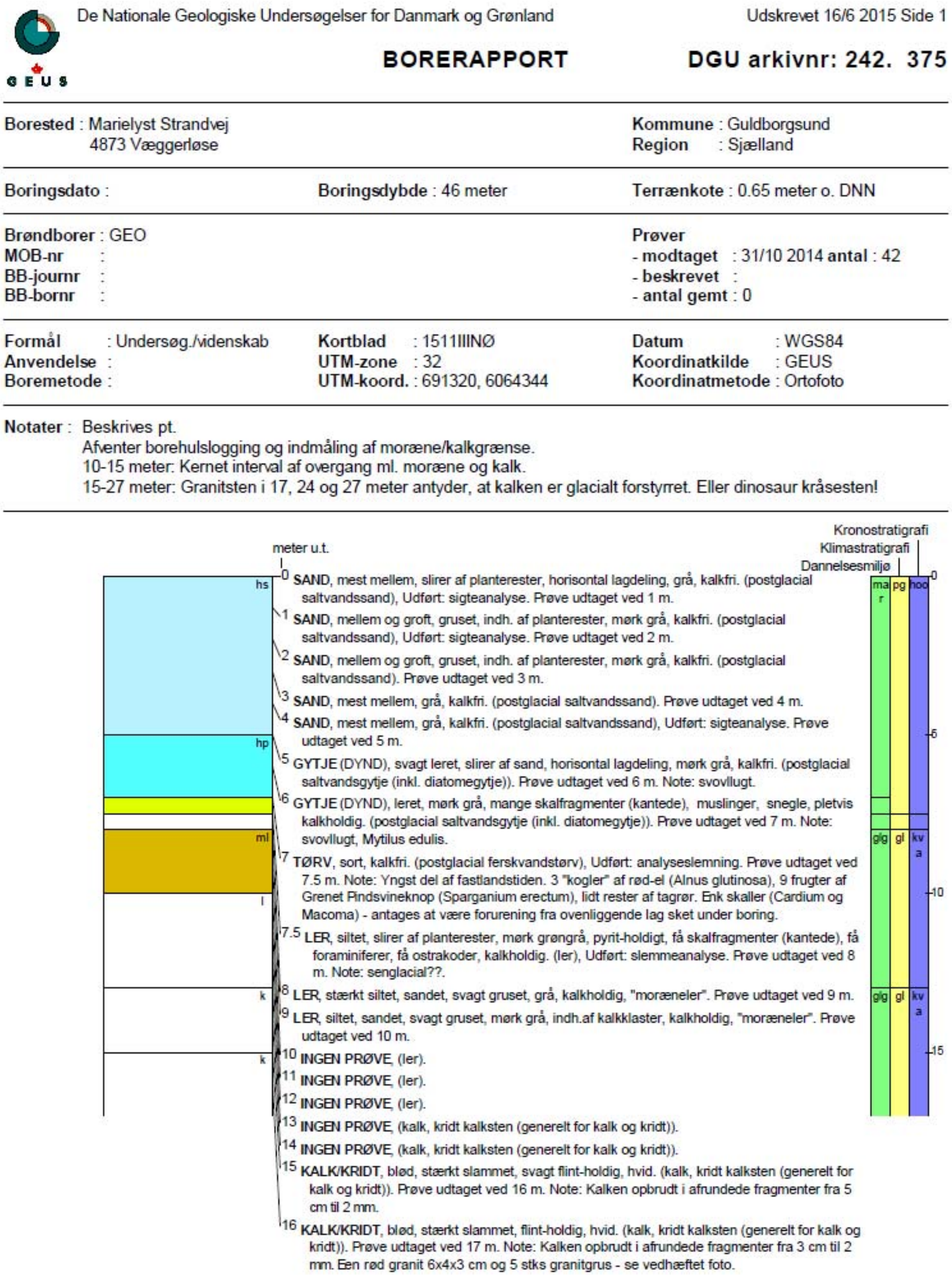

De Nationale Geologiske Undersøgelser for Danmark og Grønland — Udskrevet 16/6 2015 Side 1

GEUS

BORERAPPORT — **DGU arkivnr: 242. 375**

Borested : Marielyst Strandvej
4873 Væggerløse

Kommune : Guldborgsund
Region : Sjælland

Boringsdato :
Boringsdybde : 46 meter
Terrænkote : 0.65 meter o. DNN

Brøndborer : GEO
MOB-nr :
BB-journr :
BB-bornr :

Prøver
- **modtaget** : 31/10 2014 **antal** : 42
- **beskrevet** :
- **antal gemt** : 0

Formål : Undersøg./videnskab
Anvendelse :
Boremetode :

Kortblad : 1511IIINØ
UTM-zone : 32
UTM-koord. : 691320, 6064344

Datum : WGS84
Koordinatkilde : GEUS
Koordinatmetode : Ortofoto

Notater : Beskrives pt.
Afventer borehulslogging og indmåling af moræne/kalkgrænse.
10-15 meter: Kernet interval af overgang ml. moræne og kalk.
15-27 meter: Granitsten i 17, 24 og 27 meter antyder, at kalken er glacialt forstyrret. Eller dinosaur kråsesten!

meter u.t. — Kronostratigrafi / Klimastratigrafi / Dannelsesmiljø

hs / hp / ml / l / k / k

ma r | pg | hoo ; glg | gl | kv a ; glg | gl | kv a ; 0, 5, 10, 15

0 **SAND**, mest mellem, slirer af planterester, horisontal lagdeling, grå, kalkfri. (postglacial saltvandssand), Udført: sigteanalyse. Prøve udtaget ved 1 m.

1 **SAND**, mellem og groft, gruset, indh. af planterester, mørk grå, kalkfri. (postglacial saltvandssand), Udført: sigteanalyse. Prøve udtaget ved 2 m.

2 **SAND**, mellem og groft, gruset, indh. af planterester, mørk grå, kalkfri. (postglacial saltvandssand). Prøve udtaget ved 3 m.

3 **SAND**, mest mellem, grå, kalkfri. (postglacial saltvandssand). Prøve udtaget ved 4 m.

4 **SAND**, mest mellem, grå, kalkfri. (postglacial saltvandssand), Udført: sigteanalyse. Prøve udtaget ved 5 m.

5 **GYTJE** (DYND), svagt leret, slirer af sand, horisontal lagdeling, mørk grå, kalkfri. (postglacial saltvandsgytje (inkl. diatomegytje)). Prøve udtaget ved 6 m. Note: svovllugt.

6 **GYTJE** (DYND), leret, mørk grå, mange skalfragmenter (kantede), muslinger, snegle, pletvis kalkholdig. (postglacial saltvandsgytje (inkl. diatomegytje)). Prøve udtaget ved 7 m. Note: svovllugt, Mytilus edulis.

7 **TØRV**, sort, kalkfri. (postglacial ferskvandstørv), Udført: analyseslemning. Prøve udtaget ved 7.5 m. Note: Yngst del af fastlandstiden. 3 "kogler" af rød-el (Alnus glutinosa), 9 frugter af Grenet Pindsvineknop (Sparganium erectum), lidt rester af tagrør. Enk skaller (Cardium og Macoma) - antages at være forurening fra ovenliggende lag sket under boring.

7.5 **LER**, siltet, slirer af planterester, mørk grøngrå, pyrit-holdigt, få skalfragmenter (kantede), få foraminiferer, få ostrakoder, kalkholdig. (ler), Udført: slemmeanalyse. Prøve udtaget ved 8 m. Note: senglacial??.

8 **LER**, stærkt siltet, sandet, svagt gruset, grå, kalkholdig, "moræneler". Prøve udtaget ved 9 m.

9 **LER**, siltet, sandet, svagt gruset, mørk grå, indh.af kalkklaster, kalkholdig, "moræneler". Prøve udtaget ved 10 m.

10 **INGEN PRØVE**, (ler).

11 **INGEN PRØVE**, (ler).

12 **INGEN PRØVE**, (ler).

13 **INGEN PRØVE**, (kalk, kridt kalksten (generelt for kalk og kridt)).

14 **INGEN PRØVE**, (kalk, kridt kalksten (generelt for kalk og kridt)).

15 **KALK/KRIDT**, blød, stærkt slammet, svagt flint-holdig, hvid. (kalk, kridt kalksten (generelt for kalk og kridt)). Prøve udtaget ved 16 m. Note: Kalken opbrudt i afrundede fragmenter fra 5 cm til 2 mm.

16 **KALK/KRIDT**, blød, stærkt slammet, flint-holdig, hvid. (kalk, kridt kalksten (generelt for kalk og kridt)). Prøve udtaget ved 17 m. Note: Kalken opbrudt i afrundede fragmenter fra 3 cm til 2 mm. Een rød granit 6x4x3 cm og 5 stks granitgrus - se vedhæftet foto.

meter u.t.

17 **KALK/KRIDT**, blød, stærkt slammet, flint-holdig, hvid. (kalk, kridt kalksten (generelt for kalk og kridt)). Prøve udtaget ved 18 m. Note: Kalken opbrudt i afrundede fragmenter fra 3 cm til 2 mm.

18 **KALK/KRIDT**, blød, stærkt slammet, svagt flint-holdig, hvid. (kalk, kridt kalksten (generelt for kalk og kridt)). Prøve udtaget ved 19 m. Note: Kalken opbrudt i afrundede fragmenter fra 7 cm til 5 mm.

19 **KALK/KRIDT**, blød, stærkt slammet, svagt flint-holdig, hvid. (kalk, kridt kalksten (generelt for kalk og kridt)). Prøve udtaget ved 20 m. Note: Kalken opbrudt i afrundede fragmenter fra 5 cm til 2 mm.

20 **KALK/KRIDT**, blød, stærkt slammet, flint-holdig, hvid. (kalk, kridt kalksten (generelt for kalk og kridt)). Prøve udtaget ved 21 m. Note: Kalken opbrudt i afrundede fragmenter fra 2 cm til 2 mm.

21 **KALK/KRIDT**, blød, stærkt slammet, flint-holdig, hvid. (kalk, kridt kalksten (generelt for kalk og kridt)). Prøve udtaget ved 22 m. Note: Kalken opbrudt i afrundede fragmenter fra 1 cm til 2 mm.

22 **KALK/KRIDT**, blød, stærkt slammet, flint-holdig, hvid. (kalk, kridt kalksten (generelt for kalk og kridt)). Prøve udtaget ved 23 m. Note: Kalken opbrudt i afrundede fragmenter fra 2 cm til 2 mm.

23 **KALK/KRIDT**, blød, stærkt slammet, stærkt flint-holdig, hvid. (kalk, kridt kalksten (generelt for kalk og kridt)). Prøve udtaget ved 24 m. Note: Kalken opbrudt i afrundede fragmenter fra 1 cm til 2 mm. Een rødbrun granitsten 8x7x6 cm - se vedhæftet foto.

24 **KALK/KRIDT**, meget blød, stærkt slammet, svagt flint-holdig, hvid. (kalk, kridt kalksten (generelt for kalk og kridt)). Prøve udtaget ved 25 m.

25 **KALK/KRIDT**, meget blød, stærkt slammet, svagt flint-holdig, hvid. (kalk, kridt kalksten (generelt for kalk og kridt)). Prøve udtaget ved 26 m.

26 **KALK/KRIDT**, meget blød, stærkt slammet, flint-holdig, hvid. (kalk, kridt kalksten (generelt for kalk og kridt)). Prøve udtaget ved 27 m. Note: Een rød nærmest rund gnejs 12x12x8 cm - se vedhæftet foto.

27 **KALK/KRIDT**, meget blød, stærkt slammet, hvid, "skrivekridt". Prøve udtaget ved 28 m. Note: Fragment af Brachiopod - Carneithyris subcardinalis.

28 **KALK/KRIDT**, meget blød, stærkt slammet, hvid, "skrivekridt". Prøve udtaget ved 29 m. Note: Fragment af Brachiopod.

29 **KALK/KRIDT**, meget blød, stærkt slammet, hvid, "skrivekridt". Prøve udtaget ved 30 m.

30 **KALK/KRIDT**, meget blød, stærkt slammet, hvid, "skrivekridt". Prøve udtaget ved 31 m.

31 **KALK/KRIDT**, meget blød, stærkt slammet, hvid, "skrivekridt". Prøve udtaget ved 32 m.

32 **KALK/KRIDT**, meget blød, stærkt slammet, stærkt flint-holdig, hvid, "skrivekridt". Prøve udtaget ved 33 m.

33 **KALK/KRIDT**, meget blød, stærkt slammet, hvid, "skrivekridt". Prøve udtaget ved 34 m.

34 **KALK/KRIDT**, meget blød, stærkt slammet, flint-holdig, hvid, "skrivekridt". Prøve udtaget ved 35 m.

35 **KALK/KRIDT**, blød, stærkt slammet, stærkt flint-holdig, hvid, "skrivekridt". Prøve udtaget ved 36 m.

36 **KALK/KRIDT**, blød, stærkt slammet, stærkt flint-holdig, hvid, "skrivekridt". Prøve udtaget ved 37 m.

37 **KALK/KRIDT**, meget blød, stærkt slammet, flint-holdig, svagt leret, hvid, "skrivekridt". Prøve udtaget ved 38 m.

38 **KALK/KRIDT**, meget blød, stærkt slammet, flint-holdig, hvid, "skrivekridt". Prøve udtaget ved 39 m.

39 **KALK/KRIDT**, meget blød, stærkt slammet, svagt flint-holdig, svagt leret, hvid, "skrivekridt". Prøve udtaget ved 40 m.

40 **KALK/KRIDT**, meget blød, stærkt slammet, svagt leret, hvid, "skrivekridt". Prøve udtaget ved 41 m.

41 **KALK/KRIDT**, meget blød, stærkt slammet, flint-holdig, hvid, "skrivekridt". Prøve udtaget ved 42 m.

42 **KALK/KRIDT**, meget blød, stærkt slammet, hvid, "skrivekridt". Prøve udtaget ved 43 m.

43 **KALK/KRIDT**, hård, stærkt slammet, svagt flint-holdig, hvid, "skrivekridt". Prøve udtaget ved 44 m.

meter u.t.

44 **KALK/KRIDT**, hård, stærkt slammet, stærkt flint-holdig, hvid, "skrivekridt". Prøve udtaget ved 45 m.

45 **KALK/KRIDT**, blød, stærkt slammet, flint-holdig, hvid, "skrivekridt". Prøve udtaget ved 46 m.

46

Aflejringsmiljø - Alder **(klima-, krono-, litho-, biostratigrafi)**

meter u.t.	
0 - 7	marin - postglacial - holocæn
7 - 7.5	lakustrin - postglacial - holocæn
7.5 - 8	marin? - senglacial? - kvartær?
8 - 13	glacigen - glacial - kvartær
13 - 27	ant. glacigen - ant. glacial - ant. kvartær
27 - 46	marin - maastrichtien